Development of the timing system for the Bunch-to-Bucket transfer between the FAIR accelerators

Institution Name

GOETHE UNIVERSITÄT FRANKFURT AM MAIN

Jiaoni Bai

11th March 2017

Zusammenfassung

Widmung

Deklaration

Inhaltsverzeichnis

Abbildungsverzeichnis

Tabellenverzeichnis

Glossary

Reference RF Signal	Signal generated by the Group DDS and delivered to an individual RF cavity as a reference for the gap signal

List of Abbreviations

B2B	Bunch to Bucket
BI	Beam Instrumentation
BuTiS	Bunchphase Timing System
CCS	Central Control System
CM	Clock Master
CPU	Central Processing Unit
CR	Collector Ring
DM	Data Master
DSP	Digital Signal Processor
ESR	Experimental Storage Ring
ESR	New Experimental Storage Ring
FAIR	Facility for Antiproton and Ion Research
FEC	Front End Controller
FESA	Front-End software Architecture
FPGA	Field Programmable Gate Array
GMT	General Machine Timing
LLRF	Low-level RF
MM	Management Master
MPS	Machine Protection System
PC	Personal Computer

RESR	Recycled Experimental Storage Ring
RF	Radio Frequency
SCU	Scalable Control Unit
SM	Settings Management
TM	Timing Master
TOF	Time-of-flight
TTL	Transistor–Transistor Logic
VLAN	Virtual Local Area Network
WR	White Rabbit

List of symbols

$\alpha_b(\phi_s)$	Bucket area factor
ϕ_s	Synchronous phase
ε	Adiabaticity parameter
Q_x	Horizontal Chromaticity of SIS18
Q_y	Vertical chromaticity of SIS18
ΔQ_x	Horizontal chromatic tune shift of SIS18 due to the rf frequency modulation
ΔQ_y	Vertical chromatic tune shift of SIS18 due to the rf frequency modulation
γ_t	Transition energy
$\Delta\phi_s(t)$	Change of the synchronous phase.
C_{SIS18}	Circumference of the designed orbit of SIS18.
C_{SIS100}	Circumference of the designed orbit of SIS100.
$f_{h=1}^{SIS18}$	Revolution frequency of SIS18.
$f_{h=1}^{SIS100}$	Revolution frequency of SIS100.
$f_{h=2}^{SIS18}$	Caivity frequency of SIS18.
$f_{h=10}^{SIS100}$	Caivity frequency of SIS100.
$\Delta\phi_{shift}$	Phase shift to be achieved by the phase shift method.
$\Delta f_{rf}(t)$	Phase shift to be achieved by the phase shift method.

T	Start time of the rf frequency modulation.
t_0	Period of frequency modulation.

Kapitel 1

Introduction

1.1 FAIR project

1.2 Beam transfer systems of the FAIR accelerator

Kapitel 2

Theoretical background

Transfering bunches of particles from a synchrotron into specified buckets of another synchrotron has several underlying basic priciples. In Sec. 2.1, the basic priciples for the B2B transfer will be introduced. For FAIR, these priciples are realized based on the existing FAIR control system and LLRF system. So these two systems will be introduced in Sec. 2.2.

2.1 Introduction of the basic priciples for the B2B transfer

The energy of the beam is same before and after the B2B transfer, so the energy of the source synchrotron must first of all match that of the target synchrotron. Principally speaking, every synchrotron has its independent RF system. Then the phase advance between the bunch and the bucket must be precisely controlled before the bunch is ejected. The process of achieving the detailed phase adjustment between two RF systems is termed "RF synchronization". For the correct bucket injection, the filled buckets and the bucket to be filled must be marked. The bunch fast extraction must happen exactly one "time of flight" before the required bucket of the target synchrotron passes the injection region. The injection kicker must kick when the bucket passes the injection region. In this section, all of the B2B basic priciples will be explained.

2.1.1 Energy match

The bunch coordinates in the longitudinal phase plane of the source synchrotron, just before transfer, must be accurately controlled, according to the bucket to be filled. The target synchrotron has to center the bucket on the desired orbit [1], according to the energy of the bunch. This requirement guarantees the energy match between the bunch and bucket. The energy of a beam is determined by the 'magnetic rigidity', which is defined as the following:

$$B(t)\rho_0 = \frac{p(t)}{e} \tag{2.1}$$

where p(t) is the magnitude of the particle momentum, e is the charge of the particle, B(t) is magnetic field, and ρ_0 is the bending radius of a particle immersed in a

[1]Design orbit or injection orbit

magnetic field B(t). The ratio of p(t) to e describes the 'stiffness' of a beam, it can be considered as a measure of how much angular deflection results when a particle travels through a given magnetic field.

The bunch is transferred from the source to the target synchrotron with the same energy. So the beam has the same momentum and velocity for both synchrotrons. According to eq. 2.1, the magenetic rigidity of two synchrotrons must be matched:

$$B^{src}(t)\rho_0^{src} = \frac{p}{e} = B^{trg}(t)\rho_0^{trg} \tag{2.2}$$

Where the superscript of the symbol denotes the synchrotron, "src" represents the source synchrotron and "trg" the target synchrotron.

Besides, the rf frequency of two synchrotrons must meet the following relation.

$$C^{src}\frac{f_{rf}^{src}(t)}{h^{src}} = \beta c = C^{trg}\frac{f_{rf}^{trg}(t)}{h^{trg}} \tag{2.3}$$

where C is the circumference of the synchrotron, h the harmonic number of the rf signal and f_{rf} denotes the rf frequency at the harmonic number h, β the fraction of the particle velocity to the lightspeed.

2.1.2 Loop freeze

2.1.3 Phase difference between two RF systems

For the RF synchronization between two synchrotrons, the prerequisite is to know the phase difference between two independent RF systems.

2.1.4 RF synchronization

There are usually two methods available for the synchronization process. The synchronization is achieved by an azimuthal positioning of the bunch in the source synchrotron or the bucket in the target synchrotron. This is so-called "phase shift method". When two rf frequencies are slightly different, they are beating, perceived as periodic variations in phase difference, whose rate is the difference between the two frequencies. The synchronization is automatically achieved. This is so-called "frequency beating method". Both methods provide a time frame for the B2B transfer, within which a bunch could be transferred into a bucket with the center mismatch at least better than 1°. The time frame is called the synchronization window.

For both methods, the accompanying beam dynamics must be taken into consideration. Of the four variables, the revolution frequency f(t), B(t), p(t) and the orbit radius R(t), only two are independent. This leads to four very useful differential relations. The momentum of particle is given by

$$p(t) = e\rho_0[\frac{R(t)}{R_0}]^{1/\alpha_p}B(t) \tag{2.4}$$

where R_0 is its nominal value; and α_p, the momentum compaction factor. From eq. 2.4, the first-order total differential of p(t) is given as

$$dp(t) = \frac{e\rho_0}{\alpha_p(R_0)^{1/\alpha_p}}B(t)R(t)^{1/\alpha_p-1}dR(t) + e\rho_0[\frac{R(t)}{R_0}]^{1/\alpha_p}B(t)dB(t) \tag{2.5}$$

Dividing both sides of eq. 2.5 by p(t), we obtain

$$\frac{dp(t)}{p(t)} = \gamma_t^2 \frac{\Delta R}{R} + \frac{\Delta B}{B} \tag{2.6}$$

Now, for circular accelerators, the following general relation holds

$$f(t) = \frac{\upsilon(t)}{2\pi R(t)} \tag{2.7}$$

where $\upsilon(t)$ is its velocity. The total differential of f(t) is given by

$$df(t) = \frac{1}{2\pi}[\frac{d\upsilon(t)}{R(t)} - \frac{\upsilon(t)}{R^2(t)} dR(t)] \tag{2.8}$$

Dividing both sides of eq. 2.8 by f(t) yields

$$\frac{df(t)}{f(t)} = \frac{d\upsilon(t)}{\upsilon(t)} - \frac{dR(t)}{R(t)} \tag{2.9}$$

The fractional change in $\upsilon(t)$ is related to the fractional change in p(t):

$$\frac{dp(t)}{p(t)} = \gamma^2(t) \frac{d\upsilon(t)}{\upsilon(t)} \tag{2.10}$$

where $\gamma(t)$ is the relativistic factor, which measures the total particle energy, E(t), in units of the particle rest energy, E_0. Solving $d\upsilon(t)/\upsilon(t)$ from eq. 2.10 and substituting it into eq. 2.9 yields

$$\frac{df(t)}{f(t)} = \gamma^2(t) \frac{dp(t)}{p(t)} - \frac{dR(t)}{R(t)} \tag{2.11}$$

Replacing dp(t)/p(t) in eq. 2.11 with eq. 2.6, we have

$$\frac{df(t)}{f(t)} = \gamma^2(t) \frac{dB(t)}{B(t)} + [\frac{\gamma_t^2}{\gamma^2(t)} - 1] \frac{dR(t)}{R(t)} \tag{2.12}$$

where γ_t is the transition gamma, which is related to α_p as $\gamma_t = 1/\sqrt{\alpha_p}$. In the same way,solving dR(t)/R(t) from eq. 2.6 and substituting it into eq. 2.11, we obtain

$$\frac{df(t)}{f(t)} = (\frac{1}{\gamma^2(t)} - \frac{1}{\gamma_t^2}) \frac{dp(t)}{p(t)} + \frac{1}{\gamma_t^2} \frac{dB(t)}{B(t)} \tag{2.13}$$

2.1.4.1 Phase shift method

Based on the phase difference, the rf system of the source or target or both synchrotrons are modulated away from their nominal value for a period of time and then modulated back so that the phase shift created by the frequency modulation could compensate for the expected phase difference. After the phase shift, the bunches of the source synchrotron are synchronized with random buckets of the target synchrotron. The phase shift process must be performed adiabatically for the longitudinal emittance to be preserved.

Fig. 1 illustrates the phase shift method. The top and bottom RF signals are respectively from the source and target synchrotrons. For the phase shift method

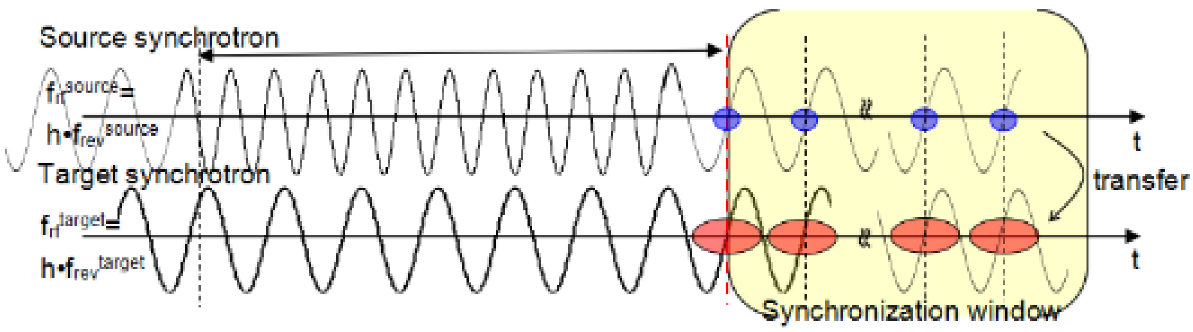

Abbildung 2.1: The illustration of the phase shift method.

two RF signals are of the same frequency. The blue dots show the position of the bunches of the source synchrotron, the red dots correspond to the bucket positions of the target synchrotron. The compensation of the time-of-flight is not drawn here. The red dashed line shows the end of the phase shift process and the beginning of the synchronization window, drawn in yellow. After the phase shift, bunches match with the random buckets.

A particular case of the B2B synchronization occurs, when the target synchrotron is empty, i.e. it did not capture any bunch yet, the phase shift can be done for the target synchrotron without adiabatical consideration (e.g. Phase jump is possible).

Now we analyze the rf frequency modulation of the phase shift from the the beam dynamics viewpoint.

- Radial excursion and momentum shift due to rf frequency modulation

  For the phase shift method, the magnetic field is not affected by the frequency modulation, so $\Delta B = 0$. By substituting $\Delta B = 0$ into eq. 2.12 and eq. 2.13, we could get respectively the accompanying radial excursion and momentum shift by the frequency modulation.

$$\frac{\Delta f}{f} = (\frac{\gamma_t^2}{\gamma^2} - 1)\frac{\Delta R}{R} \tag{2.14}$$

  and

$$\frac{\Delta f}{f} = (\frac{1}{\gamma^2} - \frac{1}{\gamma_t^2})\frac{\Delta p}{p} \tag{2.15}$$

- Transverse dynamics analysis

  The momentum spread $\Delta p/p \neq 0$ during the phase shift process causes chromaticity drift ΔQ. Q‘is the chromaticity.

$$\Delta Q = Q^{‘}\frac{\Delta p}{p} \tag{2.16}$$

- Shift of synchronous phase

  The synchronous phase deviates from 0° during the frequency modulation. From the expression of the particle momentum, p(t), given in eq. 2.4, the time derivative of p(t) can be written as

$$\frac{dp(t)}{dt} = \frac{e\rho_0 B(t)}{\alpha_p R_0^{1/\alpha_p}} R(t)^{1/\alpha_p - 1} \frac{dR(t)}{dt} + e\rho_0 (\frac{R(t)}{R_0})^{1/\alpha_p} \frac{dB(t)}{dt} \tag{2.17}$$

Now, the relationship between the rate of change in momentum of a particle, dp(t)/dt, and the force applied on it, F(t), is governed by Newton's second law:

$$\frac{dp(t)}{dt} = F(t) \tag{2.18}$$

F(t) is given by the product of the accelerating electric field, E(t), and the charge of particle, e. Substituting dp(t)/dt given in eq. 2.17 and F(t) = eE(t) into eq. 2.18, we have

$$\frac{e\rho_0 B(t)}{\alpha_p R_0^{1/\alpha_p}} R(t)^{1/\alpha_p - 1} \frac{dR(t)}{dt} + e\rho_0 (\frac{R(t)}{R_0})^{1/\alpha_p} \frac{dB(t)}{dt} = eE(t) \tag{2.19}$$

From this equation, we obtain the expression of energy gain in one turn,

$$2\pi R_0 [\frac{e\rho_0 B(t)}{\alpha_p R_0^{1/\alpha_p}} R(t)^{1/\alpha_p - 1} \frac{dR(t)}{dt} + e\rho_0 (\frac{R(t)}{R_0})^{1/\alpha_p} \frac{dB(t)}{dt}] = eV(t) sin[\phi_{s0}(t) + \Delta\phi_s(t)] \tag{2.20}$$

where V(t) is the RF accelerating voltage per turn; ϕ_{s0}, the synchronous phase in the operation with no frequency modulation; and $\Delta\phi_s(t)$, the change in the synchronous phase originating from the rf frequency modulation.

The magnetic field is not affected by the frequency change, we can assume dB(t)/dt = 0. Before the synchronizaiton, it is a stationary bucket with the synchronous phase 0°. Then, eq. 2.20 reduce to

$$2\pi R_0 [\frac{e\rho_0 B(t)}{\alpha_p R_0^{1/\alpha_p}} R(t)^{1/\alpha_p - 1} \frac{dR(t)}{dt}] = eV(t) sin[\Delta\phi_s(t)] \tag{2.21}$$

Solving $\Delta\phi_s(t)$ from eq. 2.21, we have

$$\Delta\phi_s(t) = sin^{-1}[\frac{2\pi\rho_0 B}{\alpha_p V} (\frac{R(t)}{R_0})^{1/\alpha_p - 1} \frac{dR(t)}{dt}] \tag{2.22}$$

From eq. 2.22, we know that $\Delta\phi_s(t)$ is only determined by dR(t)/dt during the frequency modulation.

- Bucket area factor

  At the flattop, the bucket is a stationary bucket with $\phi_{s0}(t) = 0$. During the frequeny modulation process, the bucket becomes a running bucket with $\Delta\phi_s(t) \neq 0$. The ratio of bucket areas of a running bucket to a stationary bucket is bucket area factor $\alpha(\Delta\phi_s)$. The bucket area factor could be estimated by [5].

$$\alpha_b(\Delta\phi_s) \approx (1 - sin(\Delta\phi_s))(1 + sin(\Delta\phi_s)) \tag{2.23}$$

- Adiabaticity analysis

  $\omega_s(t)$ is the small-amplitude synchrotron frequency given by

$$\omega_s(t) = [-\frac{\eta(t)h\omega_{rev}^2(t)eV(t)cos\phi_s(t)}{2\pi\beta^2(t)E(t)}]^{1/2} \tag{2.24}$$

  A process is called “adiabatic” when the RF parameters are changed slowly enough for the longitudinal emittance to be preserved. The condition that the parameters are slowly varying can be expressed by

$$\varepsilon = \frac{1}{\omega_s^2(t)}|\frac{d\omega_s(t)}{dt}| \ll 1 \tag{2.25}$$

  Compared with $\phi_s(t)$, all of the other variables change very slowly. $\phi_s(t) = \phi_{s0}(t) + \Delta\phi_s(t)$. From eq. (2.25) and eq. (2.24), we can write the adiabaticity parameter ε, as follows [2]:

$$\varepsilon \approx \frac{1}{2\omega_{s0}(t)}|tan\phi_s(t)\frac{d\phi_s(t)}{dt}| \tag{2.26}$$

- Constraints on the RF frequency modulation

  From eq. 2.26, we can clearly see that $\phi_s(t)$ and $d\phi_s(t)/dt$ play deterministic roles for the adiabaticity when the frequency is modulated. Now let us deduce how the rf frequency modulation affects $\phi_s(t)$ and $d\phi_s(t)/dt$. From eq. (2.14), we could get the following equation.

$$\frac{dR(t)}{dt}(\frac{\gamma_t^2}{\gamma^2} - 1)f_0 = \frac{df(t)}{dt}R_0 \tag{2.27}$$

  Substituting eq. 2.27 into eq. 2.21, we get

$$Vsin\phi_s = \frac{2\pi R_0\rho B}{f_0(\frac{1}{\gamma}^2 - \frac{1}{\gamma_t}^2)}[\frac{R(t)}{R_0}]^{(\frac{1}{\alpha_p}-1)}\frac{df(t)}{dt} \tag{2.28}$$

  Because $(R(t) - R_0)/R_0$ is about 10^{-4}, $[1 + \frac{\Delta R}{R_0}]^{(\frac{1}{\alpha_p}-1)} \approx 1$. We can get the realtion between df(t)/dt and ϕ_s from eq. 2.28.

$$Vsin\phi_s = \frac{2\pi R_0\rho B}{f_0(\frac{1}{\gamma}^2 - \frac{1}{\gamma_t}^2)}\frac{df(t)}{dt} \tag{2.29}$$

  From eq. 2.23, we know that the bucket area factor is determined by the synchronous phase change $\Delta\phi_s$. Based on eq. 2.29, we know that df(t)/dt is important for the bucket size.

  In oerder to get the relation between $d\phi_s(t)/dt$ and the frequency modulation, we get the time derivative of eq. 2.29

$$Vcos\phi_s\frac{d\phi_s}{dt} = \frac{2\pi R_0\rho B}{f_0(\frac{1}{\gamma}^2 - \frac{1}{\gamma_t}^2)}\frac{df(t)/dt}{dt} \tag{2.30}$$

  Based on the adiabaticity eq. (2.26), $d\phi_s(t)/dt$ must be existing. So $\frac{df(t)/dt}{dt}$ must be existing. It means that df(t)/dt and $\phi_s(t)$ must be continuous. In a word, there are two constraits for the rf frequncy modulation.

- The df(t)/dt of the rf frequency modulation must be small enough to guarantee the bucket size.
- The df(t)/dt of the rf frequency modulation must be continous to guarantee the continuous synchronous phase.

2.1.4.2 Frequency beating method

The frequency beating method uses the effect of two RF signals of slightly different frequencies, perceived as periodic variations in phase difference whose rate is the difference between the two frequencies. The RF frequency of the source or the target or both synchrotrons is detuned long before the ejection, then the difference between the phase of the bunch and bucket is measured. Based on the measured phase, the synchronization is realized when the phase difference of the two RF frequencies corresponds to the ideal phase difference ($\Delta\theta = 0°$). The $\Delta\theta$ is the mismatch between the bunch center and the corresponding bucket center. Because of the slightly different RF frequencies, a mismatch between the bunch and bucket centers exists. In principle, the B2B transfer requirement for FAIR allows a bunch to bucket center mismatch of 1°, which brings a symmetric time frame with respect to the time of the ideal phase difference, resulting in the maximum synchronization window for the frequency beating method, drawn in yellow, see Fig. 2.2. The red dashed line shows the time for the expected phase difference.

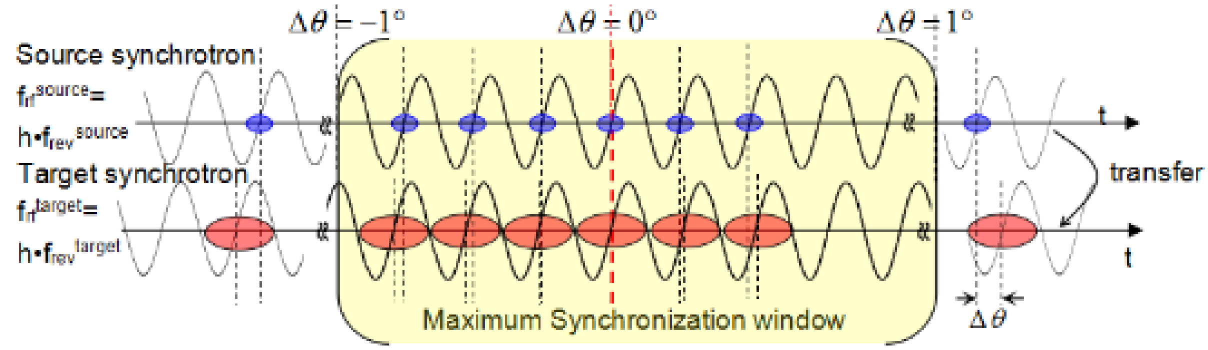

Abbildung 2.2: The illustration of the frequency beating method.

The RF frequency is detuned at the end of the ramp. During the rf frequency detune process, the magnetic field and radius excursion react and the momentum is not affected for the energy match.

- Longitudinal dynamics analysis

  Because the momentum is not affected by the frequency change, namely $\Delta \mathrm{p} = 0$, the general relation between the radial excursion and RF frequency change eq. (2.11) reduces to eq. (2.31) and the general relation between the magnetic field change and RF frequency change eq. (2.6) reduces to eq. (2.32).

$$\frac{\Delta f}{f} = -\frac{\Delta R}{R} \tag{2.31}$$

$$\frac{\Delta f}{f} = \frac{1}{{\gamma_t}^2} \times \frac{\Delta B}{B} \tag{2.32}$$

2.1.5 Bucket label

After the synchronization, the bunch is synchronized to an arbitrary RF bucket. For the proper injection, we must know which buckets are already filled and which buckets should be filled by next injection cycle. The fast extraction can only proceed when the required bucket comes.

2.1.6 Synchronization of the extraction and injection kicker

For the proper B2B transfer, the extraction and injection kickers must be synchronized with the beam.

- Extraction kicker

  Here we discuss that all bunches are extracted by one time extraction kick. The flattop is at least one revolution period. The fall time is not constrained. If there is no empty RF bucket of the ring, the rise time of the extraction kicker must be shorter than the bunch gap. If there is at least one empty RF bucket, the rise of the magnetic field could be achieved within the gap of the empty RF buckets.

- Injectin kicker

  For multi-batch injection, the rise time of the injection kicker must be shorter than the bunch gap. The flattop is determined by the length of the bunches to be injected. If all buckets must be filled, the fall time must be shorter than the bunch gap. If at least one bucket is kept empty, the fall of the magnetic field could be achieved within the gap of the empty RF buckets. If the ring needs only one time injection, the rise time is not constrained. The flattop determined by the length of the bunches to be injected. The fall time must be shorter than the bunch gap or the gap of the empty RF buckets.

2.1.7 Beam indication for the beam instrumentation

In order to observe the beams and measure related parameters for accelerators and transfer lines, the beam instrumentation (BI) equipments must be synchronized and triggered within the beam schedule. For the B2B transfer, the data acquisition for the beam instrumentation equipments should be triggered before the bunch is extracted. Sometimes they should not be triggered too early because of the limitation of sampling time. So a pre-trigger is necessary, which indicates that the bunch will be extracted/injected soon.

2.2 Infrastructures for the B2B transfer system

For the FAIR accelerator complex, synchronization of the B2B transfer will be realized by the FAIR control system and the Low-Level RF (LLRF) system. For the synchronization of LLRF system, the GMT system is complemented and linked to the Bunchphase Timing System (BuTiS).

2.2.1 FAIR control system

The FAIR control system takes advantage of collaborations with CERN in using proven framework solutions like FESA, LSA, White Rabbit, etc. It consists of the equipment layer, middle layer and application layer. The equipment layer consists of equipment interfaces, GMT and software representations of the equipment (FE-SA) Front-End System Architecture. The middle layer provides service functionality both to the equipment layer and the application layer through the IP control system network. LSA is used for the Settings Management. The application layer combines the applications for operators as GUI applications or command line tools. The application layer and the middle layer only request what the FAIR accelerator complex should do and transmit set values to the equipment layer. The actual beam production is controlled by the GMT. The GMT system is synchronized to BuTiS. The SM supplies the schedule for the GMT by LSA.

2.2.1.1 BuTiS

Bunch Phase Timing System (BuTiS) [6] [7] serves as a campus-wide clocks distribution system with subnanosecond resolution and stability over distances of several hundred meters while maintaining 100ps per km timing stability. Two BuTiS reference clocks 10 MHz and 200 MHz and a trigger identification pulse at 100 kHz are generated centrally in the BuTiS center. A star-shaped optical fiber distribution network transfers these signals to BuTiS receivers all over the FAIR campus. A BuTiS receiver and a local reference synthesizer are installed in each supply room to produce the BuTiS reference clocks, which are in phase. For this purpose, a measurement setup in the BuTiS center continuously measures the optical signal transmission delay between the BuTiS center and the different BuTiS receivers. This measurement information is used to shift the phases of the signals generated in each local reference synthesizer for the delay compensation. The main task of BuTiS is the supply of the reference clock signals for Reference RF Signal in each rf supply rooms.

2.2.1.2 GMT

The GMT [1] is contained in the equipment layer. The main tasks of the GMT system are time synchronization of more than 2000 Front-End Controllers (FEC) with nanosecond accuracy, distribution of timing messages and subsequent generation of real-time actions by the nodes of the timing system. The GMT consists of the Timing Master (TM) and the White Rabbit (WR) timing network and integrates nodes. The timing master's interface to the upper layers, e.g. online schedule monitor, is modeled as a FESA device. The timing master is a logical device, containing the data master (DM), the clock master (CM) and the management master (MM). The data master receives a schedule for the operation of the FAIR accelerator complex from the Settings Management and provides the real-time scheduler by broadcasting messages to the WR timing network, which will be received and executed by the corresponding node at the designated time. The clock master is a dedicated White Rabbit switch. It is the topmost switch layer of the WR timing network and provides the grandmaster clock which is distributed to all other nodes in the timing network. The clock master derives its clock and timestamps from the BuTiS clocks. All active components including receiver nodes and switches are registered to the management master. The management master monitor and manage the active components of the GMT system.

2.2.1.3 FESA

The real-time front-end software architecture FESA [3] is a framework used to fully integrate the large amount of front-end equipments into the FAIR accelerator control system. FESA was developed by CERN and has already been implemented into the CERN control system. FESA develops FESA classes, the equipment-type specific front-end software. For a specific type of equipments, a FESA class implementation accesses to the control interface of the equipments. The FESA class models the equipment as device, so the FESA output is called device class. One device class can instanciate several devices and thus generally handles several independent pieces of equipments. FESA provides JAVA based graphical user interfaces (GUI) to design, deploy, instantiate and test the device classes. The FEC use FESA to implement generic and equipment specific functions in form of the device classes. Interaction with the equipment is synchronized with the GMT system.

FESA (Frontend Software Architecture) is a framework developed at CERN and is now developed further in collaboration with GSI for the FAIR project. It is a toolbox to model abstract device objects where equipment's process variables (sensors and actuators) are represented as properties. The specific equipment access is implemented in C++ by the developer and is linked by the toolchain to the device model to build a so called FESA class (Fig. 4). Then, one or more FESA classes are linked to the run-time core to build an x86-Linux executable. The FESA classes provide a uniform interface via the objectproperty model and a common middle-ware to the upper layers. The device properties are set and read using synchronous or asynchronous access methods (subscription). For time multiplexed operation of the accelerators, the FESA framework supports defining multiplexed properties. Before an accelerator schedule is started the setting properties of FESA classes are presupplied by LSA [6] for all scheduled beams with specific settings accordingly. At runtime, FESA's real time software actions are triggered by timing events, the actual beam specific data is then selected based on information carried by the timing event message and send to the equipment. For the FAIR project the necessary interaction with the timing receiver is realized in a lab-specific timing library of the FESA framework.

2.2.1.4 SM

The SM is located in the middle layer of the control system. It supports off-line generation of synchrotron settings, sending these settings to all involved devices, and programming the schedule of the timing system. The SM uses the LSA (LHC Software Architecture) framework, which originates at CERN and is now developed further in collaboration with GSI for the FAIR project. The settings management is based on a physics model for accelerator optics, parameter space and overall relations between parameters and between accelerators. A standardized API allows accessing data in a common way as basis for generic client applications for all accelerators. Using the LSA-API, trim-applications can coherently modify synchrotron settings. E.g. the service generates timing constraints (e.g. ramp curve) as well as the equipment's data settings (e.g. field) for all devices derived from physics parameters (e.g. beam energy). For FAIR the framework is extended to model the overall schedule of all accelerators. Beams are described as Beam Production Chains to allow a description from beam-source to beamtarget for settings organization and data correlation.

2.2.2 LLRF system

The FAIR low-level rf (LLRF) [4] system shall be usable in the existing synchrotrons SIS18 and experimental storage ring (ESR) as well as in the FAIR synchrotrons SIS100 and SIS300 and in the storage rings collector ring (CR), new experimental storage ring (ESR), and accumulator ring (RESR).It supports fast ramp rates and large frequency span for the accleration of a variety of ion species, It supports different RF manipulations, including operation at different harmonic numbers, barrier bucket generation and bunch compression.

Cavities are driven from a supply room by a Reference RF Signal. Fig. 2.3 shows the typical cavity system with a Reference RF Signal. The cavity gets the RF signal from a local Cavity DDS (Direct Digital Synthesizer) unit, which receives RF Frequency Ramps from the Central Control System (CCS). A DSP-System (Digital Signal Processor) measures the phase between the Reference RF Signal and the gap voltage of the cavity. In the DSP system, a closed-loop control algorithm is implemented which generates frequency corrections for the local Cavity DDS. In this way, it is ensured that the phase of the gap voltage follows the phase of the reference RF signal. The Reference RF Signal distribution shown in Fig. 2.4 is located in each supply room. The virtual RF cavity is a virtual position in the synchrotron to which the Reference RF Signal corresponds. The Reference RF Signals in different supply rooms are synchronized by the BuTiS. BuTiS 200MHz and 100kHz clock signals are received by BuTiS receivers in different supply rooms in phase. In Fig. 2.4, a number of Group DDS units are located in each supply room, which are synchronized to BuTiS local reference. The Group DDS signals can be routed to the different cavity systems by a Switch Matrix. All cavities in a synchrotron could be providing with the same Group DDS signal. The cavities at different harmonic numbers could be realized by using Group DDS signals with different harmonic numbers. The Group DDS concept allows to synchronize a variety of cavities in a very flexible way.

All the cavities of SIS18 are driven from one supply room. The SIS100 cavities will be gathered in three acceleration sections, each of them is driven by a dedicated supply room.

2.2.3 MPS system

emergency kick

2.3 U^{28+} beam from SIS18 to SIS100

In this document, we use U^{28+} B2B transfer from SIS18 to SIS100 as an example. So the supercycle of U^{28+} beam of SIS18 and stacking of U^{28+} beam of SIS100 are introduced in this section.

In Fig. 2.4, SIS100 is operated at harmonic number 10, it holds 10 buckets in total, indicated by the row of ellipses in the lower part of the figure. SIS18 is operated

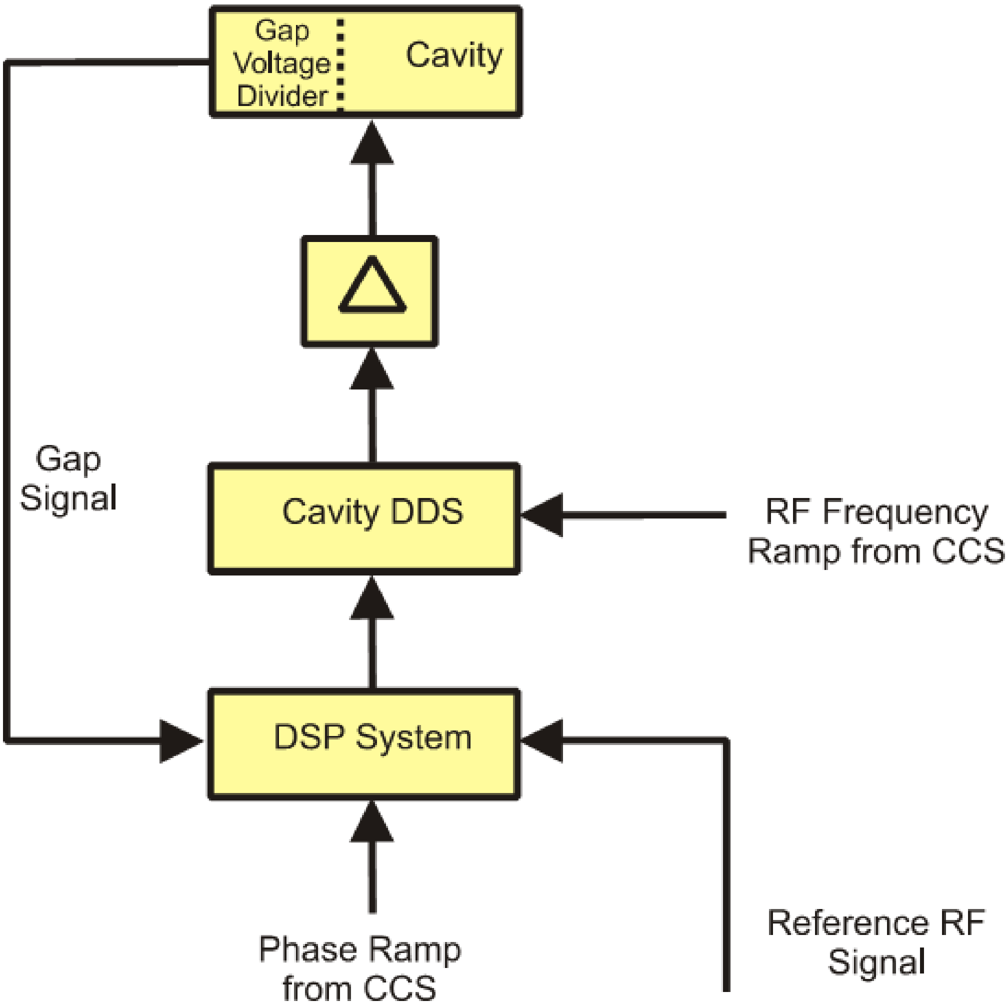

Abbildung 2.3: Local Cavity Synchronization

at harmonic number 2. The beam is accumulated using four consecutive injections of two bunches each from SIS18 into different buckets. These four consecutive cycles are called super cycle. When the injection from SIS18 is completed, 8 neighb ouring buckets in SIS100 are filled. The bucket pattern is defined as the rules of the bucket filling. After that the complete beam of SIS100 is compressed in a single bunch at harmonic number 2.

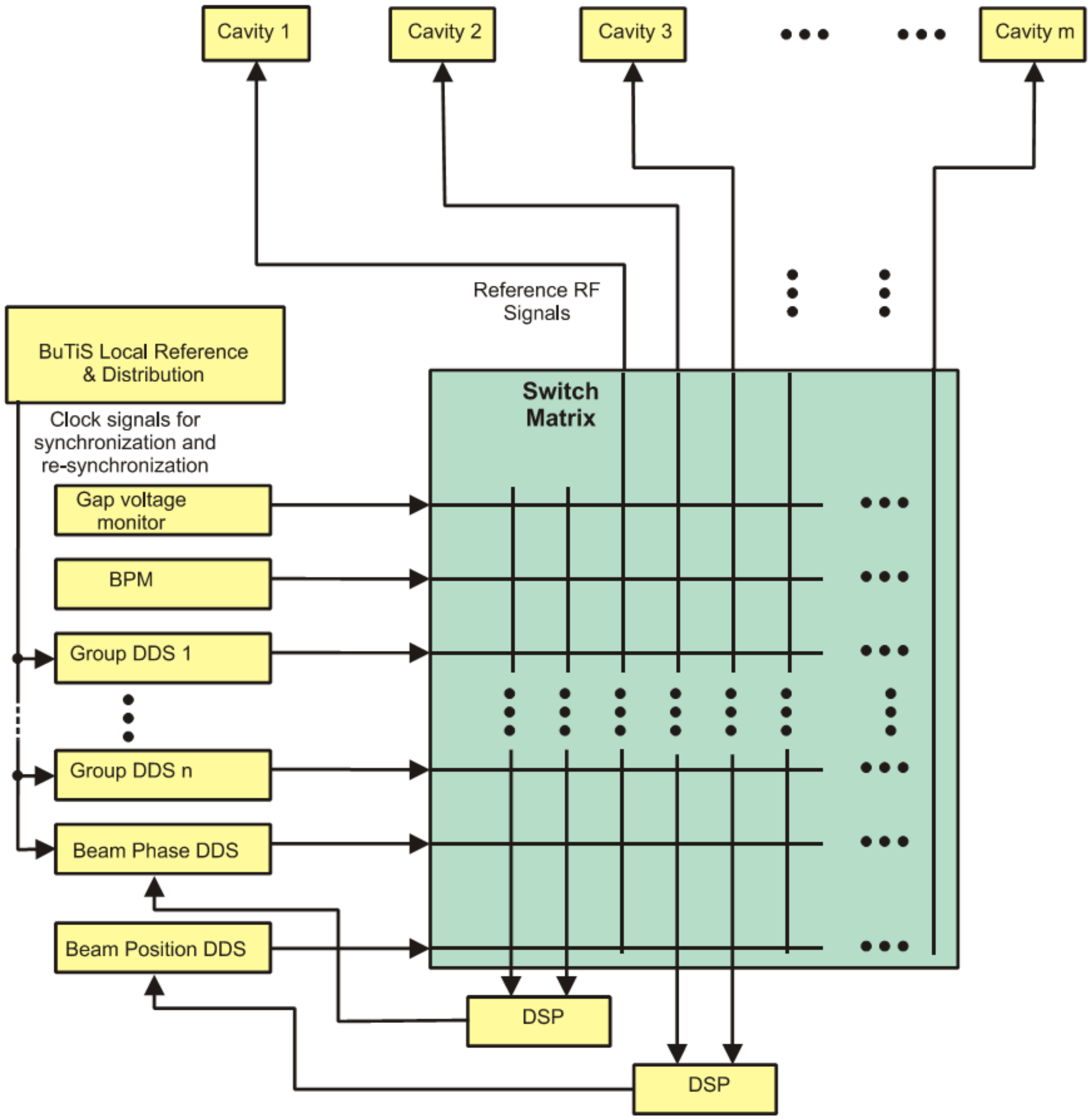

Abbildung 2.4: Reference RF Signal Distribution

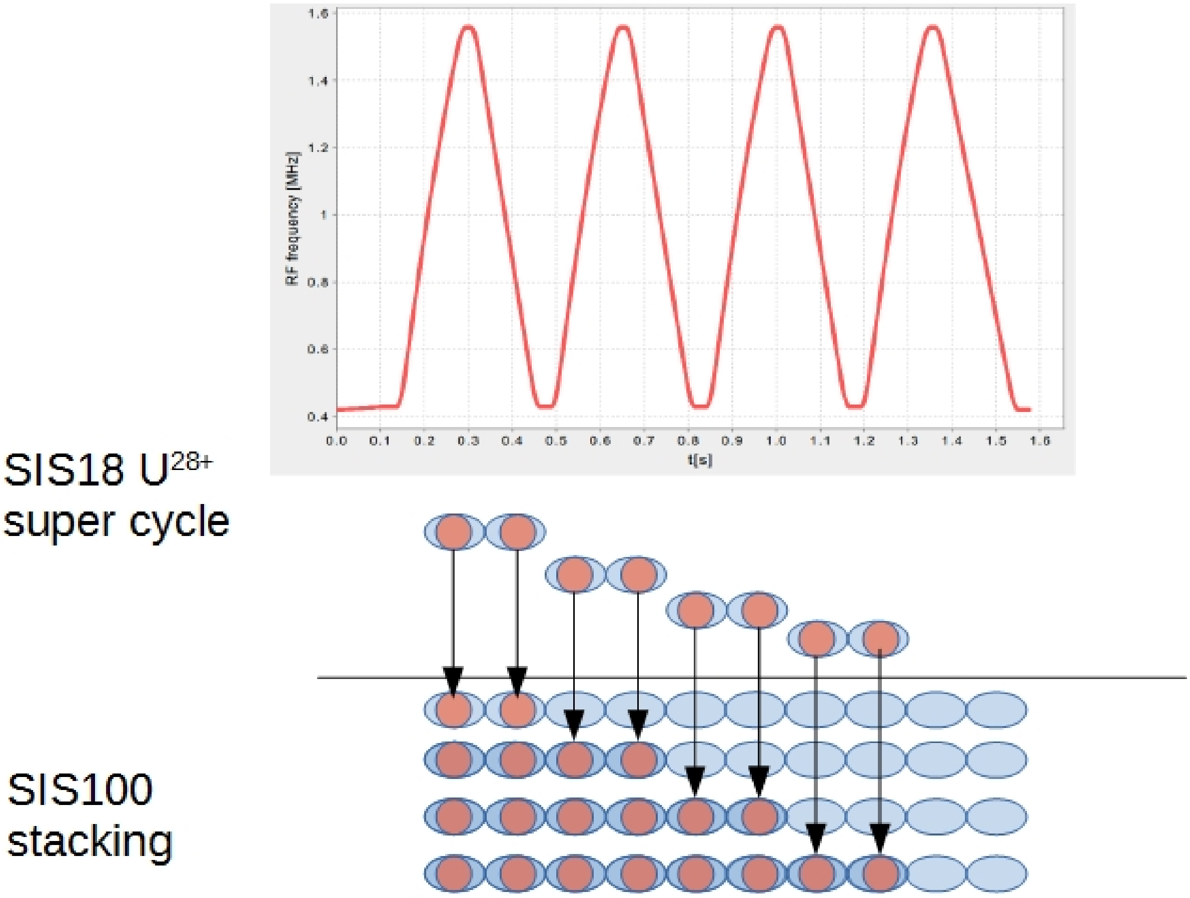

Abbildung 2.5: U^{28+} beam from SIS18 to SIS100

Literaturverzeichnis

[1] Dietrich Beck, R. Bar, Mathias Kreider, Cesar Prados, Stefan Rauch, Wesley Terpstra, and Marcus Zweig. The new White Rabbit based timing system for the FAIR facility. Proceedings of PCaPAC2012, Kolkata, India, 2012.

[2] Eizi Ezura, Masahito YOSHII, Fumihiko TAMURA, and Alexander SCHNASE. Beam-Dynamics View of RF Phase Adjustment for Synchronizing J-PARC RCS with MR or MLF, 2008.

[3] T. Hoffmann. FESA–The front-End Software architecture at FAIR. PCaPAC08, 2008.

[4] Harald Klingbeil, Ulrich Laier, Klaus-Peter Ningel, Stefan Schäfer, Christof Thielmann, and Bernhard Zipfel. New digital low-level rf system for heavy-ion synchrotrons. Physical Review Special Topics - Accelerators and Beams, 14(10), October 2011.

[5] S Y Lee. Accelerator Physics. WORLD SCIENTIFIC, Singapore, 3 edition, November 2011.

[6] Peter Moritz. BuTiS–Development of a Bunchphase Timing System. GSI Scientific Report, 2007, 2006.

[7] B. Zipfel, P. Moritz, and others. Recent Progress on the Technical Realization of the Bunch Phase Timing System BuTiS. Proc. IPAC, pages 418–420, 2011.

Kapitel 3

First idea on the B2B transfer system

3.1 Data acquisition from two synchrotrons

3.2 Coarse synchronization

3.3 Fine synchronization

After the synchronization, the bunch is synchronized to an arbitrary RF bucket. For the proper injection, we must know which buckets are already filled and which buckets should be filled by next injection cycle. So a reproduced signal at the target revolution frequency is used as the bucket marker, which labels bucket 1 of the target synchrotron. The SM knows the bucket pattern and a proper bucket offset will be applied on each injection cycle to the bucket marker. Fast extraction can only proceed when the required bucket comes. The extraction must be correctly synchronized with respect to a reference signal at the following frequency, which is called bucket marker.

3.3.1 Synchronization of the extraction and injection kicker

Because the beam of two rings are synchronized with each other, the extraction and injection are synchronized indirectly. Thyratrons are used for kicker systems at FAIR accelerator.

For FAIR project, there are several different type of kicker system. Here we introduce SIS18 extraction, SIS100 injection and extracion/emergency kicker system.

The SIS100 extraction kicker system is used for the regular extraction and the emergency extraction by bipolar operation. It consists of eight kicker magnets. Each magnet is placed between the two cable capacitors. Both cable capacitors will be charged at the same time with a high voltage DC power supply. The polarity of the magnetic field changes with the direction of the discharge current, which are controled by two thyratron switches. One polarity directs the beam into the extraction channel, the other polarity directs the beam into an underground beam dump for an emergency case. The system produces rectangular pulses with different polarities of the kicker field.

The SIS18 extraction and SIS100 injection kicker have the monopolar operation. Two cable capacitors will be charged at the same time with a high voltage DC power supply. By closing the main switch the capacitor is being discharged via the kicker magnet, which produces a rectangular kicker pulse. The pulse length can be modified by closing the dump switch in correlation with the main switch.

Fig. 3.1 shows the synchronization of the SIS18 extraction and SIS100 injection kicker for U^{28+} B2B transfer. Four batches of U^{28+} at 200 MeV/u are injected into eight out of ten buckets of SIS100. Each batch consists of two bunches. The 9th and 10th bucket may be used as bunch gap for the emergency kick. The SIS18 revolution frequency marker and SIS100 bucket markers represent time when the SIS18 bunch 1 (1st) and SIS100 bucket 1 ($\sharp$1) passes by the virtual RF cavity, which is a virtual position in the synchrotron to which the Reference RF Signal corresponds. In Fig. 3.1, the numbers correspond to the consideration of following factors for the synchronization:

- Bucket pattern ($delay_{bucket}$. E.g. $delay_{bucket}$ = One SIS18 revolution period. Bucket 3 and 4 will be filled)
- Compensation of Time-of-flight (TOF)
- Distance between the virtual RF cavity and the extraction/injection position (t_{src} and t_{trg}).
- Extraction and injection kicker delays (D_{ext} and D_{inj})

After the synchronization, the phase difference between the SIS18 and the SIS100 revolution frequency markers equals to the sum of tsrc, ttrg and TOF. The extraction kicker will be triggered by the extraction kick delay compensation, Th=1SIS1 00 + Th=1SIS18 -TOF - ttrg - Dext and the injection kicker will be triggered by the injection kick delay compensation, Th=1SIS1 00 + Th=1SIS1 8 - ttrg - Dinj. See Fig. 9. Both extraction and injection kick delay compensation values are provided by the SM.

3.3.2 Beam indication for the beam instrumentation

For the beam instrumentation system at FAIR, the data acquisition is at a sampling rate of 1GS/s and the upper bound sampling time is 100us.

The beginning of the synchronizaiton window is used for the pre-trigger.

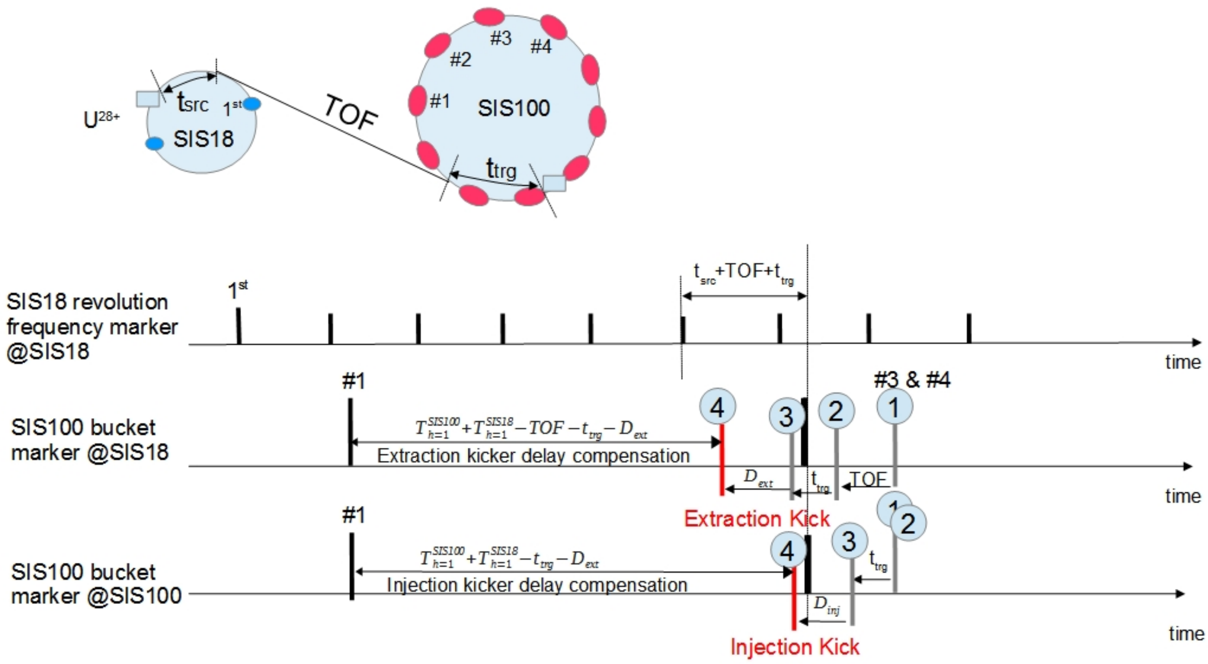

Abbildung 3.1: Synchronization of the SIS18 extraction and SIS100 injection kicker

Kapitel 4

Concept of the B2B transfer system

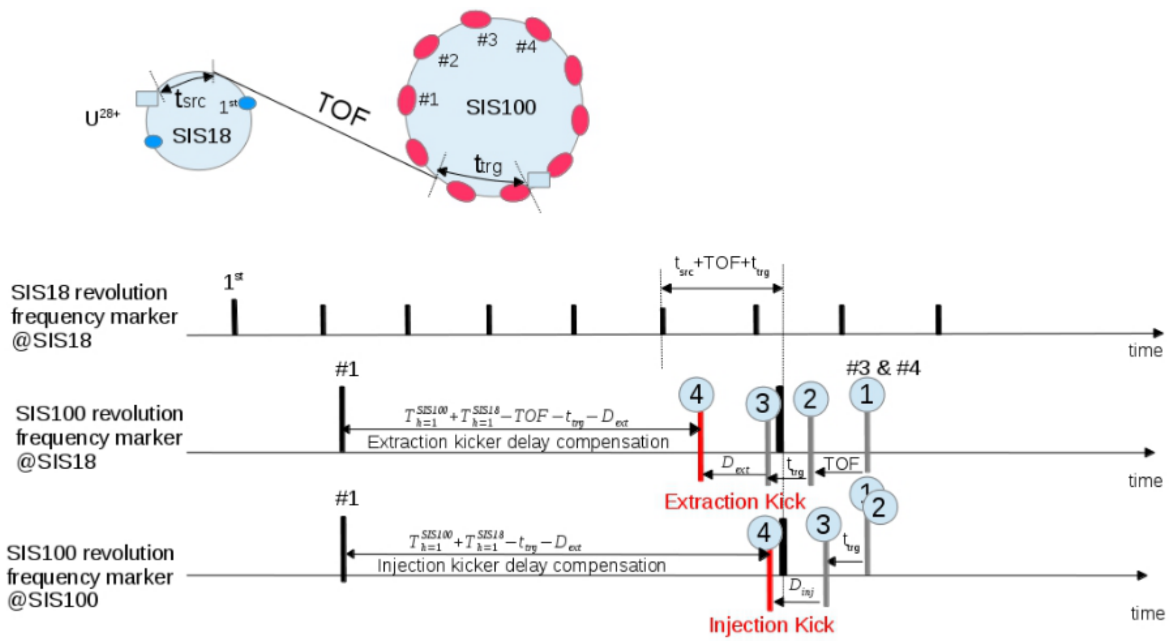

Abbildung 4.1: The illustration of U^{28+} B2B transfer from SIS18 to SIS100.

For the proper B2B transfer, the position of the bunch and bucket and the firing of the extraction and injection kicker must be precisly controlled. Fig. 4.1 illustrates the U^{28+} B2B transfer from SIS18 to SIS100. Before we explain the requirements of the B2B transfer system, some basic factors and their symbols are introduced.

- Bucket pattern ($d_{pattern}$, e.g. $d_{pattern}$ = One SIS18 revolution period. Bucket 3 and 4 will be filled).
- Compensation of Time-of-flight (TOF).
- Distance between the virtual RF cavity and the extraction/injection position (t_{src} and t_{trg}).
- Extraction and injection kicker delays (D_{ext} and D_{inj}).

In Fig. 4.1, the SIS18 and SIS100 revolution frequency marker indicate the start of the first bunch and the first bucket. The extraction and injection kicker firing are time delay on the first bars of the SIS100 revolution frequency marker at SIS18 and SIS100, which are called extraction kicker delay and injecton kicker delay. The mentioned four factors are considered on the second bars of the SIS100 revolution frequency marker. After the RF synchronization, the phase difference between the SIS18 and the SIS100 revolution frequency markers equals to the sum of t_{src}, t_{trg} and TOF.

- Extraction kick

  For the injection of the bucket 3 and 4, the extraction kicker delay for the first bar of the SIS100 revolution frequency marker is $T_{h=1}^{SIS100} + T_{h=1}^{SIS18}$, see ① at the SIS100 revolution frequency marker at SIS18. The extraction kicker must be fired TOF time eariler as the bucket passes the virtual RF cavity, so the extraction kicker delay is $T_{h=1}^{SIS100} + T_{h=1}^{SIS18} - TOF$, see ②. The extraction kicker must be fired t_{trg} time eariler as the bucket passes the virtual RF cavity, so the extraction kicker delay is $T_{h=1}^{SIS100} + T_{h=1}^{SIS18} - TOF - t_{trg}$, see ③. The extraction kicker must be fired D_{ext} time eariler for the kicker preparasion, so the extraction kicker delay is $T_{h=1}^{SIS100} + T_{h=1}^{SIS18} - TOF - t_{trg} - D_{ext}$, see ④.

- Injection kick

  For the injection of the bucket 3 and 4, the injection kicker delay for the first bar of the SIS100 revolution frequency marker is $T_{h=1}^{SIS100} + T_{h=1}^{SIS18}$, see ① at the SIS100 revolution frequency marker at SIS100. The injection kicker must be fired t_{trg} time eariler as the bucket passes the virtual RF cavity, so the injection kicker delay is $T_{h=1}^{SIS100} + T_{h=1}^{SIS18} - t_{trg}$, see ③. The injection kicker must be fired D_{inj} time eariler for the kicker preparasion, so the injection kicker delay is $T_{h=1}^{SIS100} + T_{h=1}^{SIS18} - t_{trg} - D_{inj}$, see ④.

In order to realize the B2B transfer above, we specify how the basic B2B principles are realized for FAIR in Sec. 4.1. The standard procedure is defined and described in Sec. 4.2. The Sec. 4.3 and 4.4 describe the U^{28+} B2B process from SIS18 to SIS100 with both synchronization methods.

4.1 Realization of the basic B2B principles

In this section, I will explain how the basic B2B principles are realized based on the FAIR control system and LLRF system. Fig. 4.2 shows the topology of the B2B transfer system.

4.1.1 RF difference between two RF system

In order to get the phase difference between two RF systems, we make use of a shared reference signal at both source and target synchrotrons, which is called a Synchronization Reference Signal. It is with the fixed frequency and always in the same phase at two synchrotrons. It is a sine wave, whose frequency is a multiple of the BuTiS T0 100 kHz and whose zero-crossing is aligned with T0 edges in order to ensure the synchronization of the Synchronization Reference Signal in different

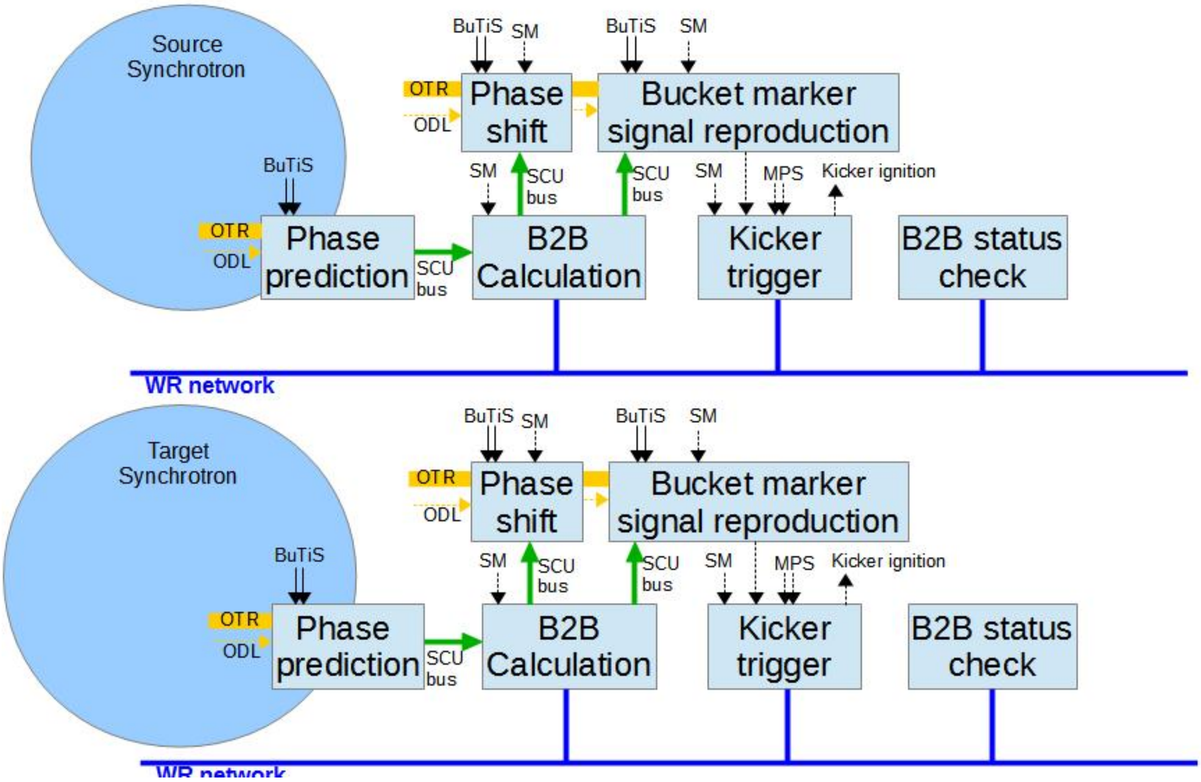

Abbildung 4.2: The topology of the B2B transfer system

synchrotrons. Fig. 4.3 shows the realization of the phase difference between two RF systems. Fig. 4.3 (a) and (b) illustrate the phase measurement and prediction in the source and target synchrotrons. The red sine waves in Fig. 4.3 (a) and (b) represents the Synchronization Reference Signals (100 kHz) in two synchrotrons and the black waves the Reference RF signals (200 kHz). The phase difference $\Delta\varphi1$ between the Reference RF Signal and the Synchronization Reference Signal is measured at the source synchrotrons and $\Delta\varphi2$ at the target synchrotron. The phase measurement is performed synchronously to an internal clock, which is represented by the blue dots. Based on a series of the phase difference measurements, the phase difference at T0 edges $\psi1$ and $\psi2$ are predicted in every synchrotron, which is represented by the red diamonds in Fig. 4.3. More details about the phase measurement and phase prediction, please see Tibo's thesis. Becasue the phase prediction is synchronized with T0 clocks and the Synchronization Reference Signal's phase is 0° aligns at T0 edges, $\psi1$ and $\psi2$ are the phase of the Reference RF Signals. In order to get the phase difference between two rf systems $\psi1$ - $\psi2$, the phase of the target synchrotron is transferred to the source synchrotron.

4.1.2 RF synchronization

The B2B transfer system for FAIR is available for both the phase shift and frequency beating methods, see Sec. 2.1.3.

- RF synchronization with the phase shift method

  Eq. 4.1 gives the relation between the required phase shift and the frequency

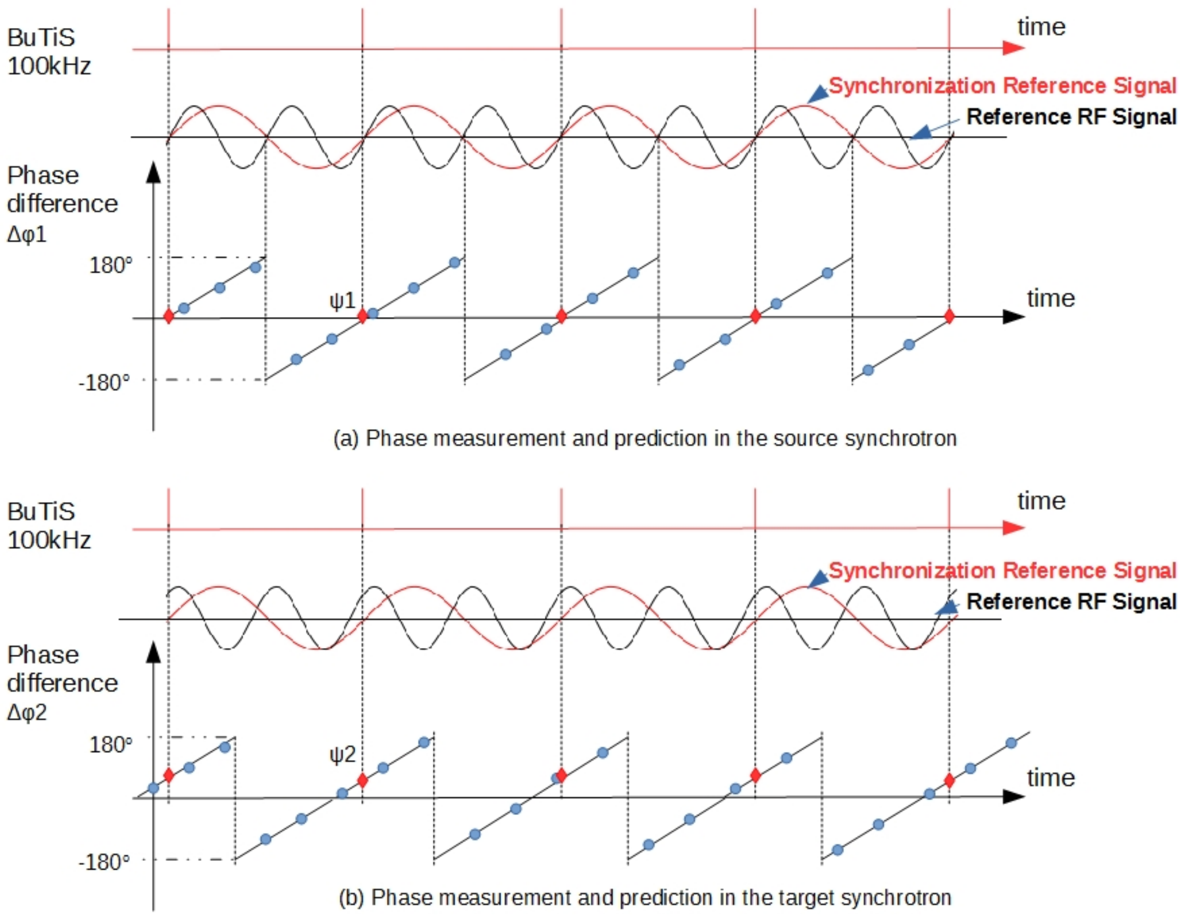

Abbildung 4.3: The realization of the phase difference between two synchrotrons

modulation.

$$\Delta\phi = 2\pi \int_{t_0}^{t_0+T} \Delta f(t)dt \tag{4.1}$$

The required phase shift is determined by the frequency offset Δf and the duration of the frequency modulation T. The phase shift must be executed adiabatically in order to guarantee the bucket size and continuous synchronous phase, see Sec. 2.1.3.1. We introduce a phase shift of up to $\pm 180°$ in the phase shift for FAIR. With the two criteria, a normalized frequency modulation profile $f_{normalized}$ for 180° can be precalculated. The actual frequency modulation profile f_{actual} is decided by the normalized frequency modulation profile and the required phase shift, see eq. 4.2. The B2B transfer system for FAIR uses the fixed duration of the frequency modulation.

$$\frac{\Delta\phi}{180°} = \frac{f_{actual}}{f_{normalized}} \tag{4.2}$$

Fig. 4.4 shows the normalized and actual frequency modulation profiles and the corresponding phase shift. The magenta profile is the normalized profile $f_{normalized}$ with the phase shift of 180°. The blue is $1/2f_{normalized}$ with the phase shift of 90° and the green is $1/3f_{normalized}$ with 60°. The Reference RF Signal is phase shifted by means of either frequency (Fig. 4.4 (a)) or phase

(Fig. 4.4 (b)) modulation. The phase shifted Reference RF Signal is routed to the different cavity systems by a Switch Matrix to realize the phase shift of all cvities on the synchrotron.

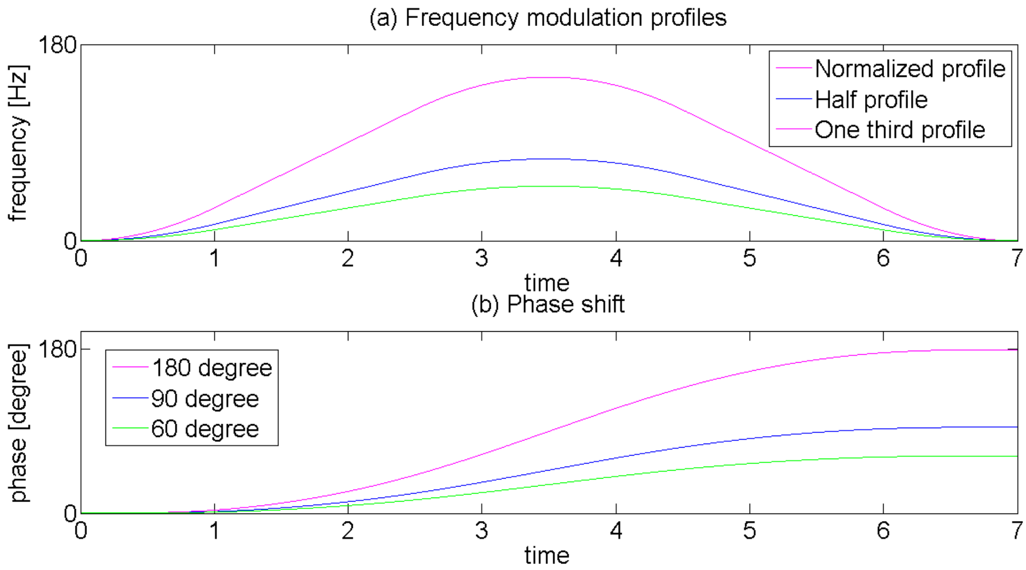

Abbildung 4.4: The normalized frequency modulation profile and the actual profile

A particular case of the B2B synchronization occurs, when the target synchrotron is empty, i.e. it did not capture any bunch yet, the phase shift can be done for the target synchrotron without adiabatical consideration (e.g. Phase jump is possible).

- RF synchronization with the frequency beating method

  The ratio of the circumference between many pair of machines in FIAR is not a perfect integer, e.g. SIS18 and ESR (injection orbit), SIS100 and CR, CR and HESR. so the RF synchronization is automatically with the frequency beating method. For the pairs with the perfect interger ratio of the circumference, e.g. SIS18 and SIS100, we detune the rf frequency of the source synchrotron by modifying the magnetic field and radial excursion to get the frequency beating.

4.1.3 Bucket label

The B2B transfer system for FAIR needs the bucket label not only at the rf flattop, but also during the whole acceleration cycle. The former is used for the normal extraction and injection and the latter is used for the emergency kick of SIS100.

- Bucket label for the normal extraction and injection

  For the bucket label for the normal extraction and injection, three steps are necessary. Fig. 4.5 shows these three steps for the U^{28+} bucket label of SIS100.

  - Step 1. Frequency correction

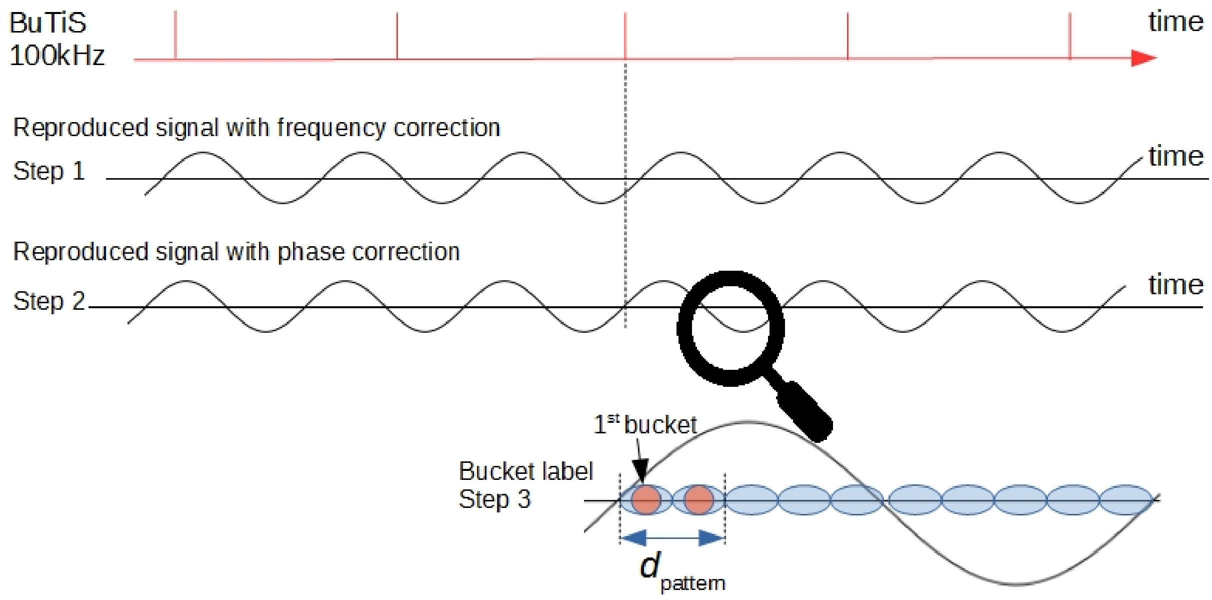

Abbildung 4.5: The realization of the bucket label for the normal extraction and injection.

A signal with the same frequency as the Reference RF Signal at the flat-top of the target synchrotron (e.g. RF revolution frequency of SIS100) is produced, which is called the reproduced signal. For the B2B transfer system for FAIR, the zero-crossing of the reproduced signal alwasys indicates the start of the 1st bucket.

- Step 2. Phase correction

  For the phase synchronization with the bucket, the bucket label signal must do phase correction at a specified T0 edge.

- Step 3. Bucket label

  The SM manages the bucket pattern with the parameter of $d_{pattern}$ on the reproduced signal. In Fig. 4.5, the 3rd and 4th buckets will be filled with $d_{pattern}$.

• Bunch gap label for the emergency extraction

Only for SIS100 emergency procedure, the bunch gap label is important during the whole acceleration cycle. There are two steps for the realization of the bunch gap label, see Fig. 4.6.

- Step 1. The reproduced signal is directly distributed from the switch matrix, which synchronizes with the Reference RF Signal in frequency and phase.

- Step 2. Bunch gap label

  The SM informs the bunch gap with the parameter of $d_{pattern}$ on the reproduced signal during the whole acceleration cycle. In Fig. 4.6, the 9th

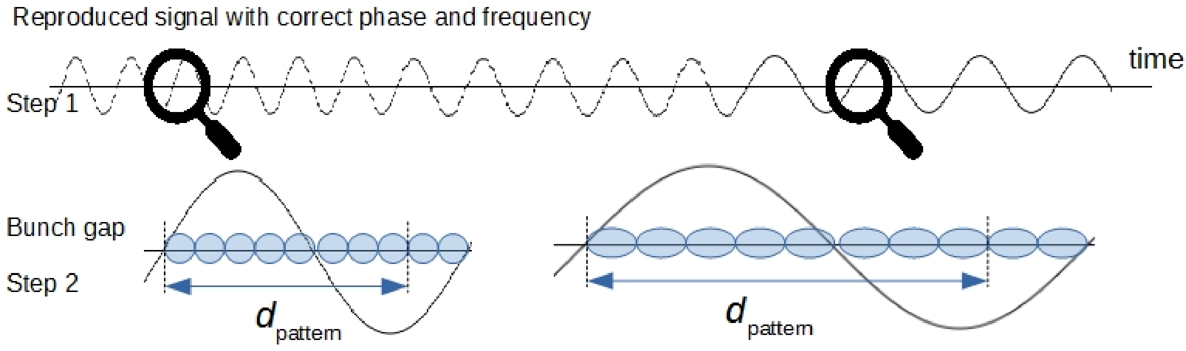

Abbildung 4.6: The realization of the bunch gap for the emergency extraction.

and 10th buckets services as the bunch gap. The $d_{pattern}$ is with variable value, which is preloaded from the SM and applied to the reproduced signal on T0 edges.

4.1.4 Synchronization of the extraction and injection kicker

For the normal B2B extraction/injection, the synchronization window is a gating signal, within which the first reproduced signal will be selected. The extration and injection kicker are synchronized with the bunch and bucket by the extration and injection kicker delay compensation. If the inhibit signal of MPS is off, the kicker delay compensation must be considered for the kicker synchronization. The extraction kicker will be triggered by the extraction kick delay compensation, $T_{h=1}^{SIS100} + T_{h=1}^{SIS18} - TOF - t_{trg} - D_{ext}$ and the injection kicker will be triggered by the injection kick delay compensation, $T_{h=1}^{SIS100} + T_{h=1}^{SIS18} - t_{trg} - D_{inj}$, see Fig. 4.1. Both extraction and injection kick delay compensation values are provided by the SM. If the inhibit signal is on, the normal injection and extraction trigger signals will be blocked.

For the SIS100 emergency kick, the extraction delay compensation is calculated by $T_{h=1}^{SIS100} + d_{pattern} - t_{emg} - D_{emg}$. t_{emg} is the distance between the virtual RF cavity and the emergency extraction position and D_{emg} the emergency kicker delay.

4.1.5 Beam indication for the beam instrumentation

Two timing frames will be send from the source synchrotron to the DM.

- Timing frame TGM_SYNCH_WIN

  This time frame indicates the start of the synchronization window for the beam instrumentation.

- Timing frame TGM_B2B_STATUS

  The source synchrotron is responsible for examining the status of the B2B transfer system and transferring the status and the actual beam injection time to the DM by TGM_B2B_STATUS. If all components of the B2B transfer system work correctly and the B2B transfer process is accomplished, the status bit is ‘0‘. Otherwise it is ‘1‘. For this purpose, The source synchrotron shall do simple checking based on the extraction/injection trigger time, the actual beam extraction/injection kick time. E.g. Source trigger time < actual beam extraction time.

4.2 Basic procedure of the B2B transfer system for FAIR

Fig. 4.7 illustrates the basic prodedure of the B2B transfer with two different synchronization scenarios. The top part shows the chronological steps with the frequency beating method, while the bottom part shows the steps with the phase shift method. The emergency kickers can be triggered at any time during the acceleration cycle by the MPS. The yellow region shows the synchronization window. The purple region shows the valid time for the emergency kicker.

The B2B transfer process basically needs to follow six steps:

1. The DM announces the B2B transfer and freezes the beam-phase loop, when required.

2. The two synchrotrons measure the rf phase locally.

3. The source synchrotron gathers the measured rf phase from the target synchrotron.

4. The source synchrotron calculates the synchronization window with the kicker delay and sends it to both synchrotrons and to the DM. Besides, it reproduces the bucket label signal at the source synchrotron. For the phase shift method, the source synchrotron generally achieves the phase shift. But when the target synchrotron is empty, the phase shift is achieved at the target synchrotron.

5. The trigger signal is generated for the kickers with the delay compensation.

6. The kicker electronics fire the kickers.

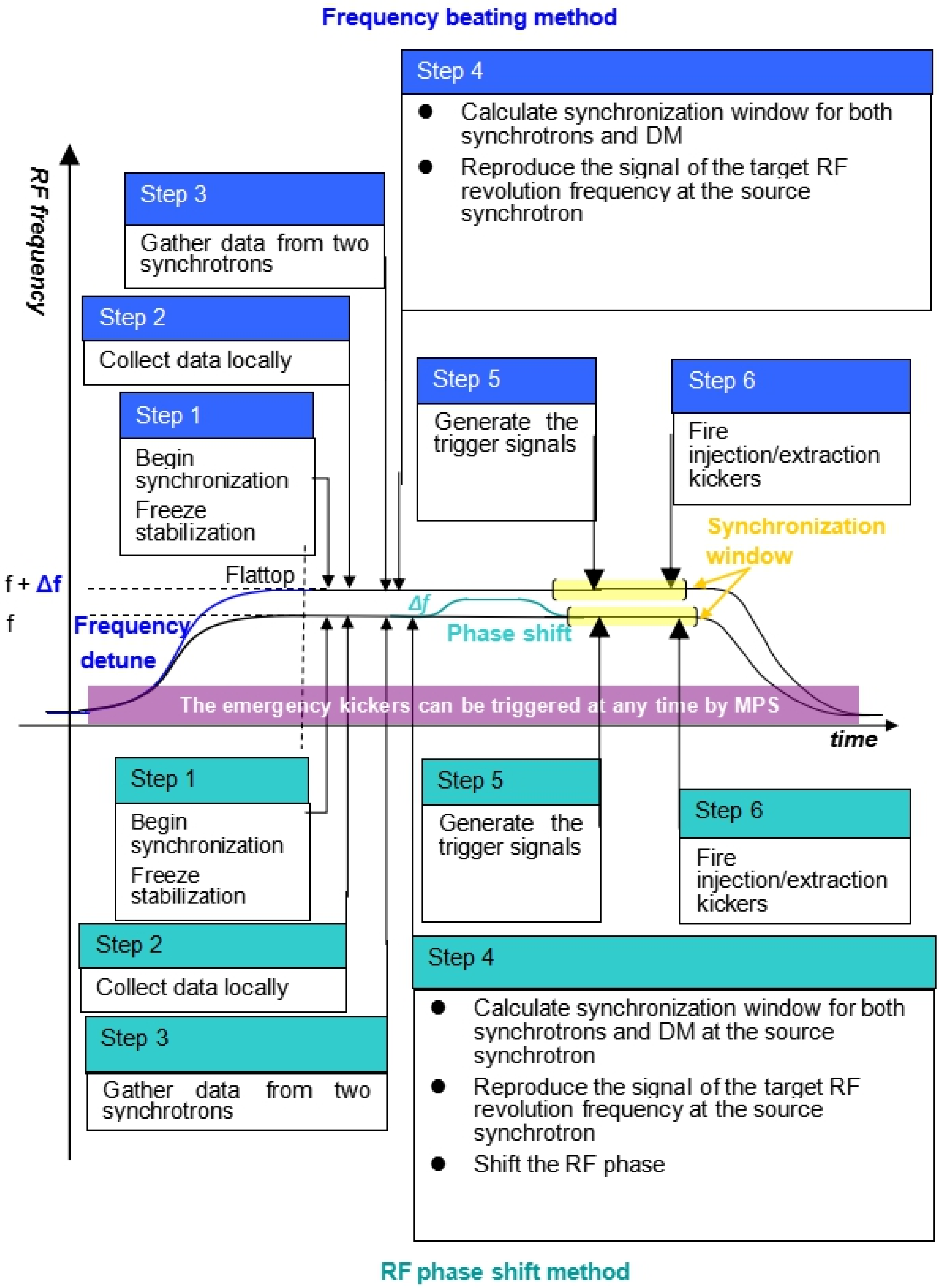

Abbildung 4.7: The procedure for the B2B transfer within one acceleration cycle. Shown are the frequency beating method (blue, top) and the phase shift method (green, bottom).

4.3 Description of the U^{28+} B2B process from SIS18 to SIS100 with the phase shift method

Here the U^{28+} at 200 meV/u B2B transfer from SIS18 to SIS100 will be described in detail. Fig. 4.8 shows one SIS18 U^{28+} super cycle. It consists of four SIS18 cycles. Each cycle produces two bunches. From SIS18, four cycles of the U^{28+}, each of two bunches, are injected into eight out of ten buckets of SIS100. In each SIS18 cycle, the beam is accelerated to the top energy after injection. At the RF flattop, the synchronization is implemented with the phase shift method by modulating rf frequency. The ratio of the SIS100 circumference to the SIS18 circumference is 5. The harmonic number for SIS100 is 10 and for SIS18 is 2. At the flattop, the RF cavity frequency of SIS18 is 1.572 MHz as that of SIS100, so the phase difference between two RF signals is almost constant. To perform the B2B transfer, this phase difference must be corrected to compensate for the required phase difference by phase shift. The frequency ramp at the start and end of the SIS18 frequency modulation must be performed adiabatically. Here we use a parabola rf frequency modulation, more details please see Sec. 5.1.1. Then the time for a phase shift of 180° is 7 ms.

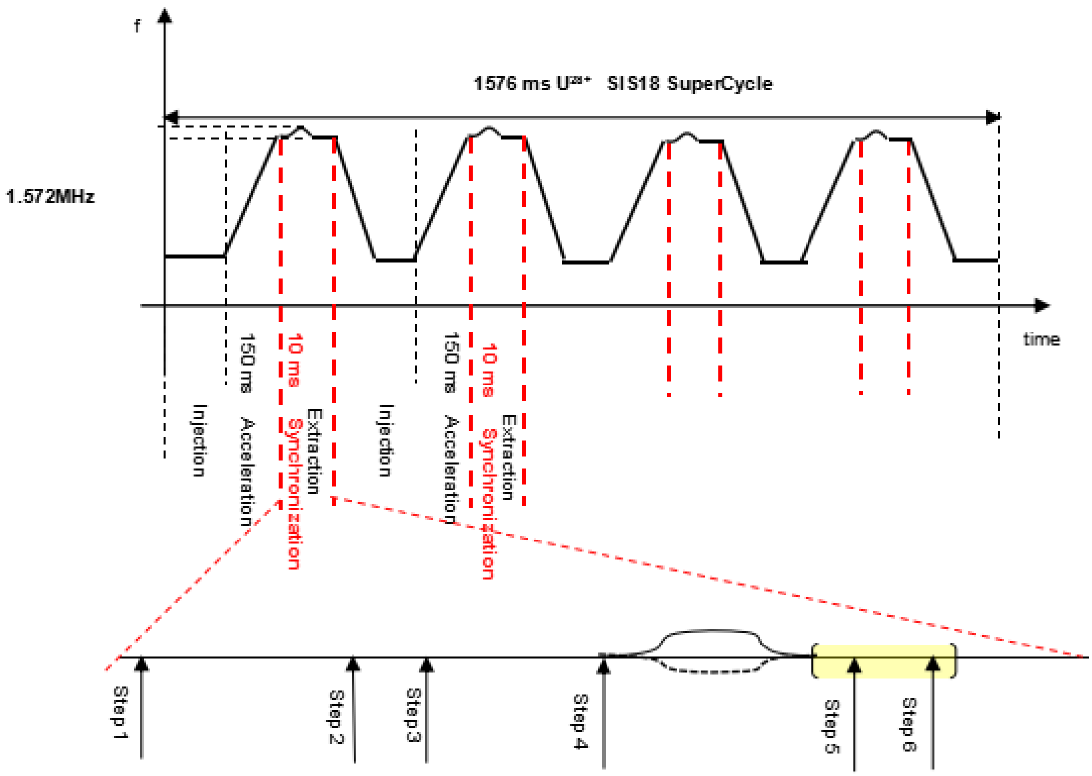

Abbildung 4.8: The B2B transfer inside one SIS18 U^{28+} Super Cycle with the phase shift method.

4.4 Description of the U^{28+} B2B process from SIS18 to SIS100 with the frequency beating method

For the frequency beating method of the U^{28+} at 200 meV/u B2B transfer from SIS18 to SIS100, we assume to detune 200 Hz for the SIS18 rf signal during the acceleration ramp. The beating frequency is 200 Hz and the synchronization period is 5 ms.

Fig. 4.9 illustrates the standard synchronization process with the frequency beating method. In order to guarantee that eight sequential buckets will be filled by eight bunches.

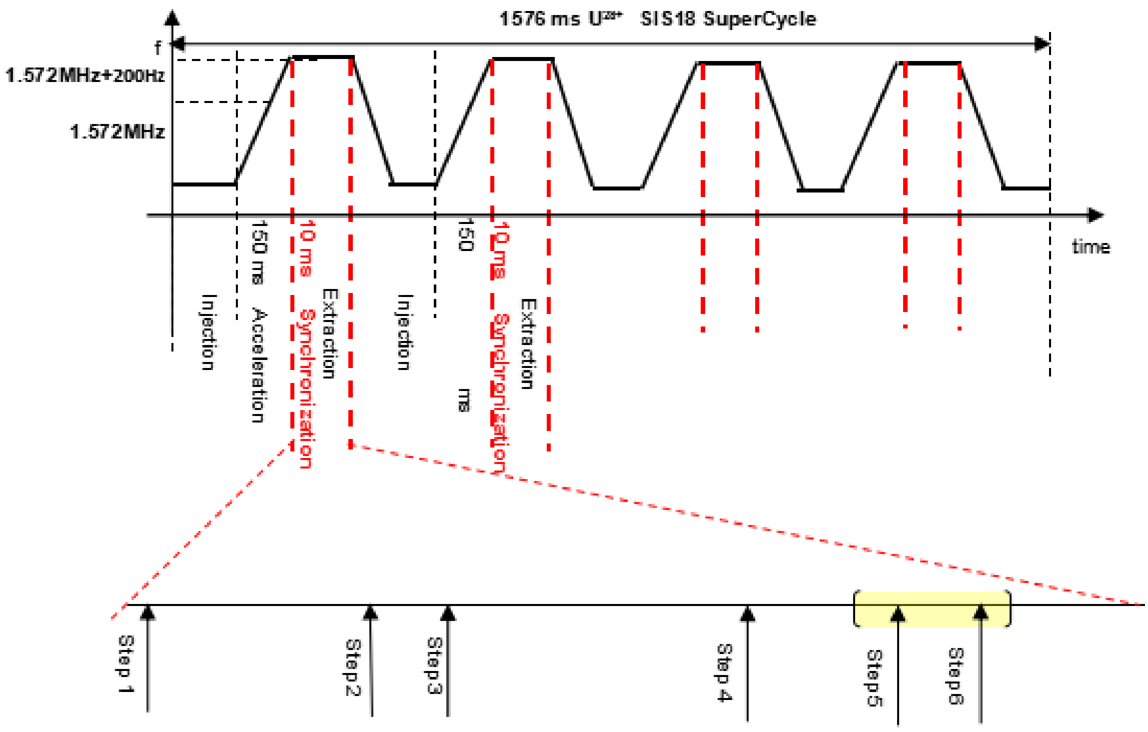

Abbildung 4.9: The B2B transfer inside one SIS18 U^{28+} Super Cycle with the frequency beating method.

Kapitel 5

Realization and systematic investigation of the B2B transfer system

This chapter concentrates on the realization and systematic investigation of the B2B transfer system. Both the phase shift and frequency beating synchronization methods are analyzed from the beam dynamic viewpoint. The GMT and kicker systematic considerations of the B2B transfer are investigated. Besides, the test setup from the timing aspect is built. All the analysis are based on U^{28+} B2B transfer from SIS18 to SIS100.

5.1 Investigation of two synchronization methods for U^{28+} B2B transfer from SIS18 to SIS100 from the beam dynamics viewpoint

This section analyzes the phase shift and frequency beating methods from the beam-dynamics viewpoint for the synchronization of SIS18 with SIS100. In this chapter, the circumference of SIS18 and SIS100 are denoted by C_{SIS18} and C_{SIS100}, the revolution frequency by $f_{h=1}^{SIS18}$ and $f_{h=1}^{SIS100}$ and the rf frequency by $f_{h=2}^{SIS18}$ and $f_{h=10}^{SIS100}$. Since SIS18 and SIS100 harmonic number are 2 and 10, the relationship between the revolution and rf frequencies are $f_{h=2}^{SIS18} = 2f_{h=1}^{SIS18}$ and $f_{h=10}^{SIS100} = 10f_{h=1}^{SIS100}$. Since C_{SIS100} is five times as long as C_{SIS18}, we could get the relation $f_{h=1}^{SIS18}$=$5f_{h=1}^{SIS100}$ and $f_{h=10}^{SIS100}$=$f_{h=2}^{SIS18}$.

5.1.1 Phase shift method

To achieve a required phase shift, the RF frequency is modulated away from the norminal value for a period of time and modulated back. Let $\Delta\phi_{shift}$ be the phase shift to be achieved and $\Delta f_{rf}(t)$ the RF frequency variation to accomplish it; then,

$$\Delta\phi_{shift} = 2\pi \int_{t_0}^{t_0+T} \Delta f_{rf}(t)dt \tag{5.1}$$

where T is the period of frequency modulation and t_0 is the time at which the modulation begins. To make the frequency modulation effective, the stabilization system, beam-phase loop, must be frozen before the modulation begins.

The following four examples of frequency modulation are analyzed. Case (1) rectangle modulation, Case (2) triangular modulation, Case (3) sinusoidal modulation and Case (4) parabolic modulation. Here I assume the phase shift must be achieved within 7ms. These frequency modulations are shown in Fig. 5.1. All the four modulations give the same phase shift, $\Delta\phi_{shift} = \pi$, which is proved by substituting each form of $\Delta f_{rf}(t)$ into eq. 5.1 and performing integration. Fig. 5.2 shows the time derivation of four rf frequency modulations, which are smaller than the maximum time derivative of rf frequency during the acceleration ramp 64Hz/ms for the adiabaticity consideration. The acceleration ramp is an adiabatical process.

Case (1)

$$\Delta f_{rf}(t) = \begin{cases} 50Hz/ms \times (t - t_0) & t_0 + 0 < t \leq t_0 + 2ms \\ 100Hz & t_0 + 2 < t \leq t_0 + 5ms \\ 100Hz - 50Hz/ms \times (t - t_0) & t_0 + 5ms < t \leq t_0 + 7ms \end{cases} \tag{5.2}$$

Case (2)

$$\Delta f_{rf}(t) = \begin{cases} \frac{10^3}{7\times 3.5} Hz/ms \times (t - t_0) & t_0 + 0 < t \leq t_0 + 3.5ms \\ \frac{10^3}{7} Hz - \frac{10^3}{7\times 3.5} Hz/ms \times (t - t_0 - 3.5ms) & t_0 + 3.5ms < t \leq t_0 + 7ms \end{cases} \tag{5.3}$$

Case (3)

$$\Delta f_{rf}(t) = \frac{10^3}{14} Hz \times (1 - cos(\frac{2\pi}{7} rad/ms \times (t - t_0))) \quad t_0 + 0 < t \leq t_0 + 7ms \tag{5.4}$$

Case (4)

$$\Delta f_{rf}(t) = \begin{cases} 30Hz/ms^2 \times (t - t_0)^2 & t_0 + 0 < t \leq t_0 + 1ms \\ 30Hz + 60Hz/ms \times (t - t_0 - 1ms) & t_0 + 1ms < t \leq t_0 + 2.5ms \\ 30Hz/ms^2 \times [5ms - (t - t_0 - 3.5ms)^2] & t_0 + 2.5ms < t \leq t_0 + 4.5ms \\ 30Hz + 60Hz/ms \times (6ms - t - t_0) & t_0 + 4.5ms < t \leq t_0 + 6ms \\ 30Hz/ms^2 \times [7ms - (t - t_0)]^2 & t_0 + 6ms < t \leq t_0 + 7ms \end{cases} \tag{5.5}$$

5.1.1.1 Longitudinal dynamic analysis for the simulation

In this section, the average radial excursion, the relative momentum shift, synchronous phase, bucket size and adiabaticity of four rf frequency modulations are analyzed.

- Average radial excursion

  The average radial excursion is calculated for the four cases of rf frequency modulations by eq. (2.14). Fig. 5.3 shows the calculation result. The maximum average radial excursion of case (1) is 2.93×10^{-6} at the flat of the frequency modulation and that of case (2), case (3) and case (4) are 4.17×10^{-6}, 4.18×10^{-6} and 4.38×10^{-6} at the midpoint 3.5ms of the frequency modulations. The maximum tolerant radial excursion of SIS18 is $\pm 2.4 \times 10^{-4}$. From the view point of the average radial excursion, four cases of rf frequency modulations are available.

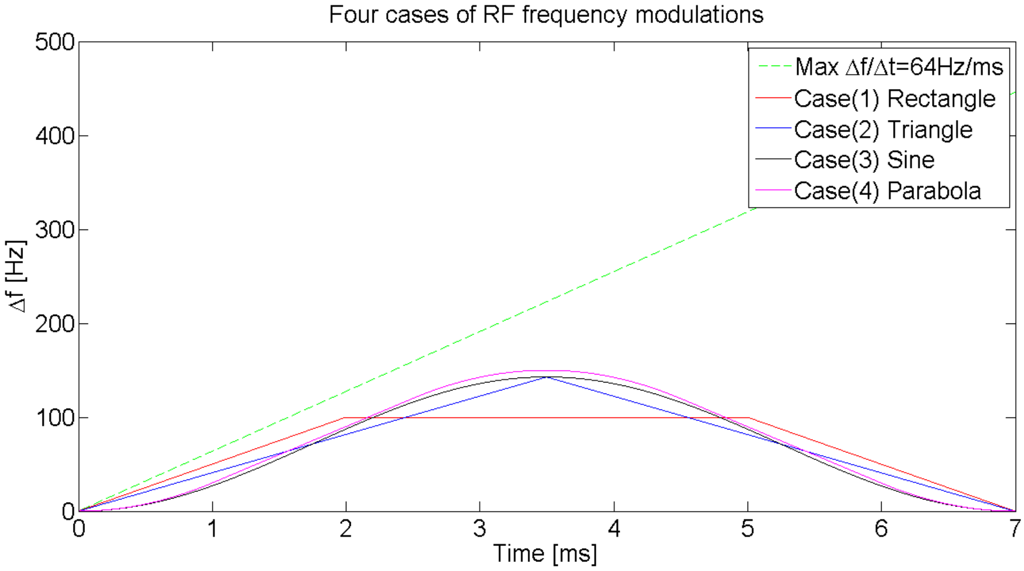

Abbildung 5.1: Examples of RF frequency modulation.

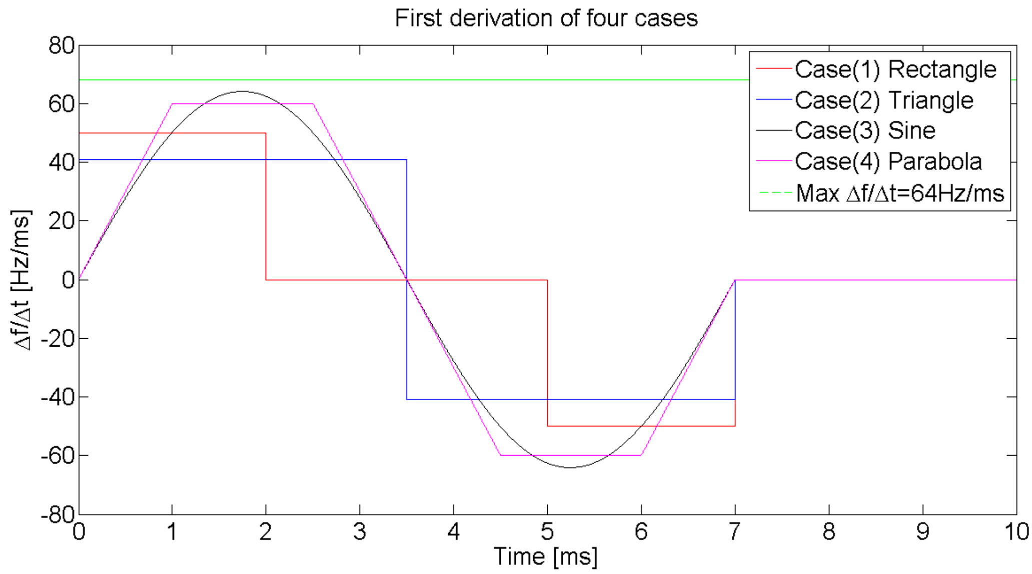

Abbildung 5.2: Time derivation of four modulations

- Relative momentum shift

  The relative momentum shift is calculated for the four cases of rf frequency modulations by eq. (2.15). Fig. 5.4 shows the calculation result. The maximum relative momentum modulation of case (1) is 9.83×10^{-5} at the flat of the frequency modulation and that of case (2), case (3) and case (4) are 1.38×10^{-4}, 1.40×10^{-4} and 1.48×10^{-4} at the midpoint 3.5ms of the frequency modulations. The maximum tolerant relative momentum shift of SIS18 is ± 0.008. From the view point of the relative momentum shift, four cases of rf frequency modulations are available.

- Synchronous phase

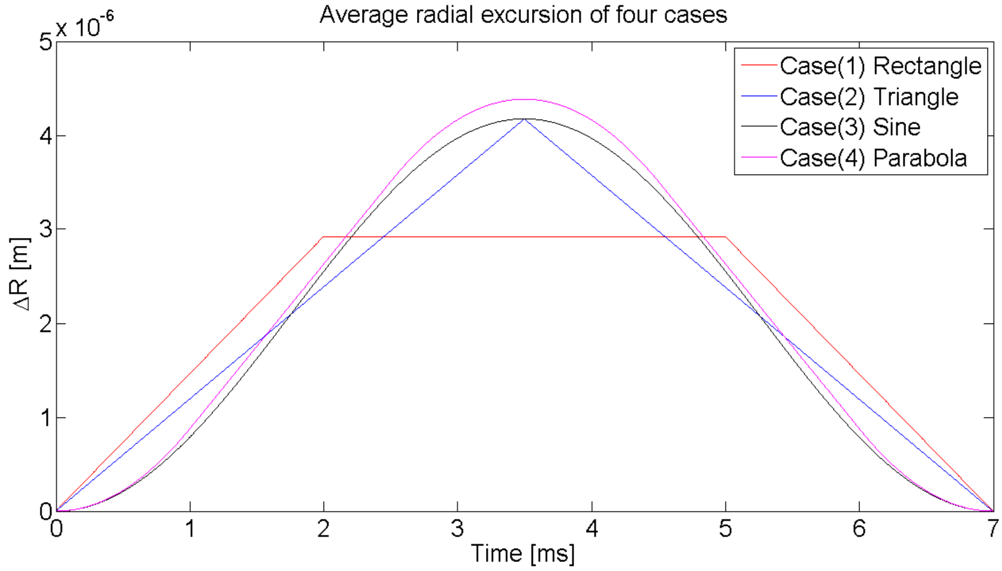

Abbildung 5.3: Average radial excursions of four cases.

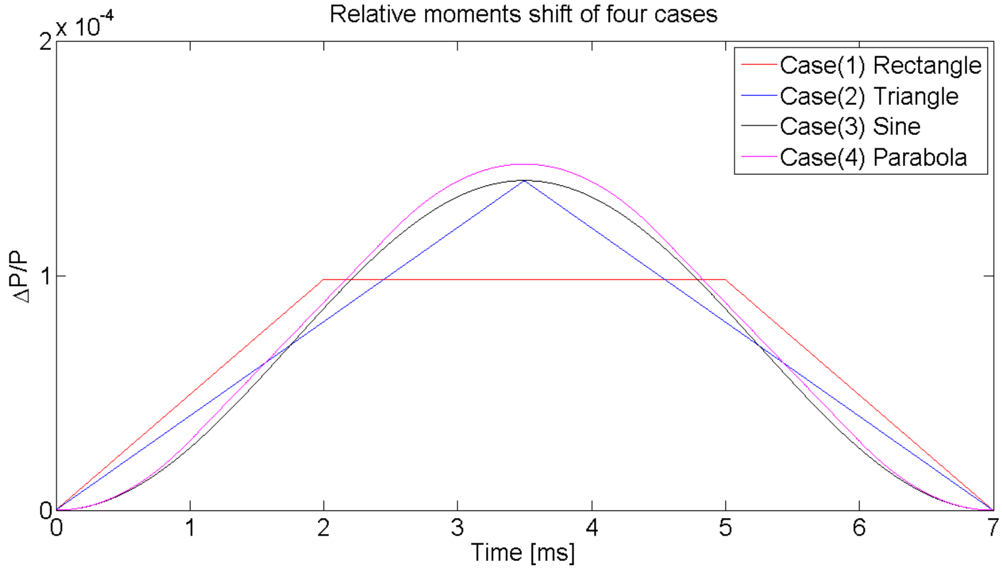

Abbildung 5.4: Relative momentum shift of four cases.

The rf frequency modulations make the synchronous phase deviate from the norminal value 0°. Fig. 5.5 shows the changes in the synchronous phase, $\Delta\phi_s$ (t). It is calculated by introducing values into eq. (**??**). For case (1), the phase jumps in $\Delta\phi_s(t)$ appear at the start and end of the frequency modulation, and at two points where the slope of modulation changes from upward to flat and from flat to downward. For case (2), the phase jumps in $\Delta\phi_s(t)$ appear at the start and end of the frequency modulation, and at the midpoint where the slope of modulation changes from upward to downward. For case (3) and (4), the synchronous phase $\Delta\phi_s(t)$ during the modulations are continuous. The phase jumps are dangerous for the beam to follow. From the view point of the synchronous phase, four cases of rf frequency modulations are available.

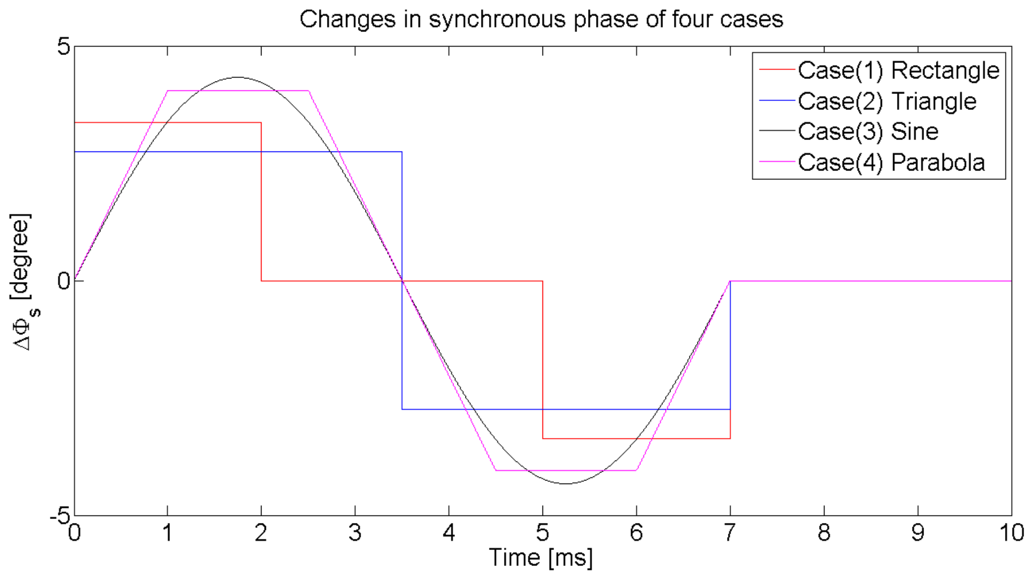

Abbildung 5.5: Changes in synchronous phase of four cases

- Bucket size

  The bucket area factor $\alpha_b(\phi_s)$ varies during rf frequency modulations. Before the modulations, the synchronous phase ϕ_s=0° and $\alpha_b(0°) = 1$. By introducing the changes in synchronous phase into eq. (5.6), we get the ratio of bucket areas of a running bucket to the stationary bucket for four cases, see Fig. (5.6).

$$\alpha_b(\phi_s) \approx (1 - sin\phi_s)(1 - sin\phi_s) \tag{5.6}$$

  The running bucket size is lager than 88% of the stationary bucket for case (1). The running bucket size is lager than 90% of the stationary bucket for case (2). The running bucket size is lager than 86% of the stationary bucket for case (3) and (4). From the viewpoint of the bucket size, four rf frequency modulations are available.

- Adiabaticity

  By substituting the values of $d\Delta\phi_s(t)/dt$ obtained from Fig. 5.5 and the other appropriate values into eq. **??**, we can calculate the adiabaticity parameter, ε, for the case (3) and (4), see Fig. 5.7. For the case (1) and (2), however, we cannot calculate $d\Delta\phi_s(t)/dt$ from $d\Delta\phi_s(t)$ shown in Fig. 5.5, because $d\Delta\phi_s(t)$ changes discontinuously.

  For case (4), the maximum of ε, 0.000059, occurs at 1ms, 2.5ms, 4.5ms and 6ms. Form Fig. 5.5, we could see the change of the synchronous phase $d\Delta\phi_s(t)/dt$ is big but smoothly at these time points. For case (3), the maximum of ε is 0.000030. So the frequency modulation is adiabatical for case (3) and (4).

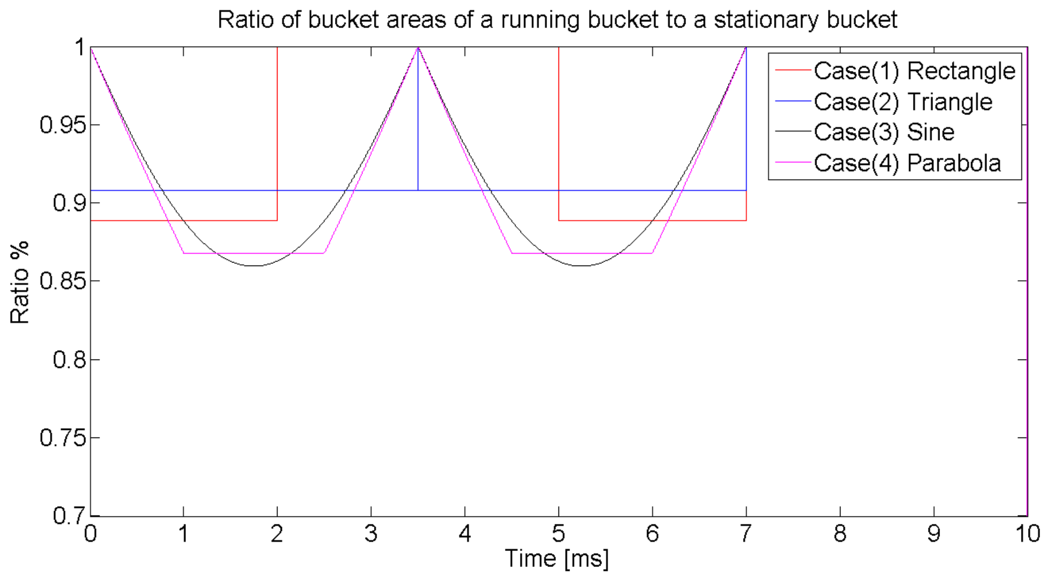

Abbildung 5.6: Ratio of bucket areas of a running bucket to the stationary bucket of four cases

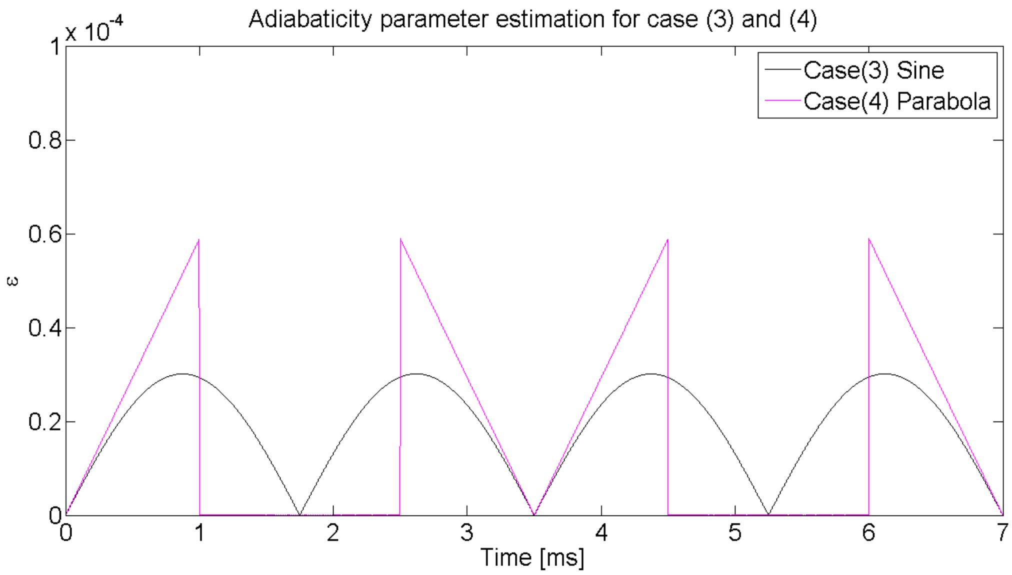

Abbildung 5.7: Adiabaticity parameter estimation of case (3) and (4)

5.1.1.2 Transverse dynamics analysis for the simulations

From Fig. 5.4, we could get the maximum momentum shift for four cases, 9.83×10^{-5}, 1.38×10^{-4}, 1.40×10^{-4} and 1.48×10^{-4}. For SIS18, the chromaticity Q_x and Q_y is 4.17 and 3.4. Substituting chromaticity and maximum momentum shift into eq. 2.16. We could get the chromatic tune shift ΔQ_x and ΔQ_y during rf modulations for four cases.

Case (1)

$$\Delta Q_x = 4.17 \times 9.83 \times 10^{-5} = 4.10 \times 10^{-4} \tag{5.7}$$

$$\Delta Q_y = 3.4 \times 9.83 \times 10^{-5} = 3.34 \times 10^{-4} \tag{5.8}$$

Case (2)

$$\Delta Q_x = 4.17 \times 1.38 \times 10^{-4} = 5.75 \times 10^{-4} \tag{5.9}$$

$$\Delta Q_y = 3.4 \times 1.38 \times 10^{-4} = 4.69 \times 10^{-4} \tag{5.10}$$

Case (3)

$$\Delta Q_x = 4.17 \times 1.40 \times 10^{-4} = 5.84 \times 10^{-4} \tag{5.11}$$

$$\Delta Q_y = 3.4 \times 1.40 \times 10^{-4} = 4.76 \times 10^{-4} \tag{5.12}$$

Case (4)

$$\Delta Q_x = 4.17 \times 1.48 \times 10^{-4} = 6.17 \times 10^{-4} \tag{5.13}$$

$$\Delta Q_y = 3.4 \times 1.48 \times 10^{-4} = 5.03 \times 10^{-4} \tag{5.14}$$

The chromatic tune shift for four cases are significantly small, which could be negligible.

5.1.2 Frequency beating method

In the case of the frequency beating method, we guarantee the extraction and injection energy always match, which means that the momentum is not affected by the frequency detune, namely $\Delta p = 0$, So the frequency beating method has no influence on the transverse dynamics.

5.1.2.1 Longitudinal dynamics analysis of the frequency beating for SIS18

For the frequency beating method, the rf frequency de-tune is done accompanying with the RF ramp. Accepting to decentre the orbit by 8mm for the SIS18

$$\frac{\Delta R}{R} = \pm 2.4 \times 10^{-4} \tag{5.15}$$

From eq. 2.31 and and eq. 2.32, the RF frequency and the magnetic field change at the U^{28+} extraction energy 200MeV/u ($\gamma_t = 5.8$) are

$$\frac{\Delta f}{f} = \pm 2.4 \times 10^{-4} \tag{5.16}$$

$$\frac{\Delta B}{B} = \frac{\Delta f}{f} {\gamma_t}^2 = \pm 8.1 \times 10^{-3} \tag{5.17}$$

where the maximum RF frequency de-tune is approximate to 370 Hz at 1.57 MHz for the U^{28+}. Fig. 5.8 shows the rf frequency derivation during the rf ramp. In the simulation, I assume that the rf frequency is detuned at 0.2756s with 6.08×10^6Hz/s, see blue rectangle in Fig. 5.8. For the sake of simplicity, 200 Hz is used as the rf frequency detune. SIS18 needs approximate 33us to reach 200 Hz with 6.08×10^6Hz/s.

From eq. 2.31 and eq. 2.32, we could get the corresponding radial excursion and the magnetic field change during the detune process. The maximum radial excursion is -1.27×10^{-4} at 33us of the rf detune process. The maximum magnetic field change is 4.3×10^{-3} at 33us of the rf detune process.

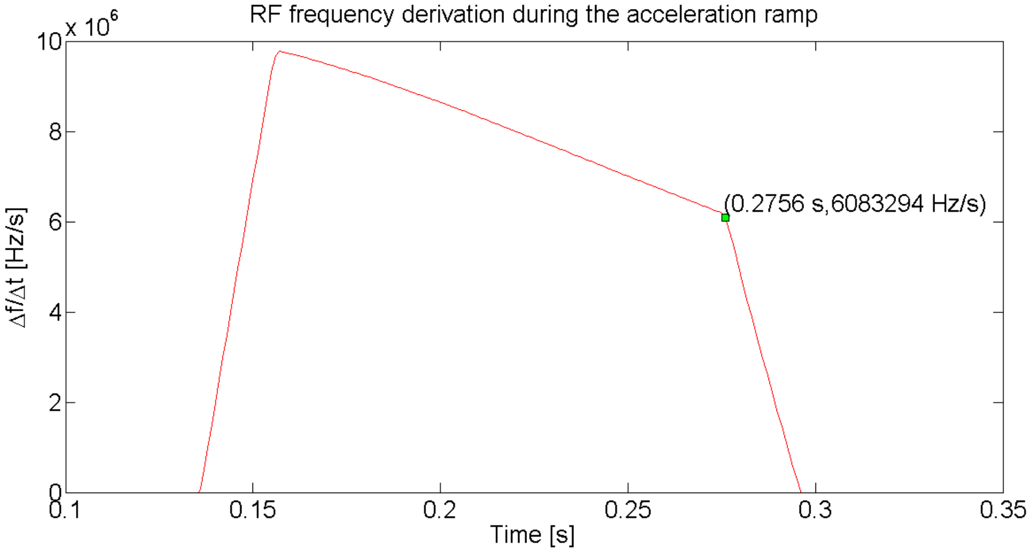

Abbildung 5.8: RF frequency derivation of the U^{28+} rf ramp

5.2 GMT systematic investigation for the B2B transfer system

GMT system plays a very important role for the B2B transfer system. It is responsible for the data collection, merging and redistribution. The main task of the data merging is the calculation of the synchronization window, within which the bunch could be injected into the correct bucket with the bunch to bucket center mismatch better than 1°. The data collection and redistribution make use of the WR network, so the measurement of the WR network latency is necessary.

5.2.1 Calculation of the synchronization window

According to the predicted phase advance, we could calculate the fine time for the alignment of two RF Reference Signals for both the phase shift and frequency beating methods. This time is called "best estimate of alignment" and denoted by t_{best}. See Fig. 5.9. Because of the uncertainty of the phase advance prediction and rf frequency modulation, the fine alignment lies between t_{best} - δt_{best} and t_{best} + δt_{best}. δt_{best} is called the uncertainty of the alignment and [t_{best} - δt_{best}, t_{best} + δt_{best}] is called "probable range of alignment". In Sec.5.2.1.1 and Sec.5.2.1.2, the calculation of the best estimation of alignment and the probable range of alignment for the phase shift and frequency beating method will be explained. The probable range of alignment is within the synchronization window. For the correct selection of the same revolution frequency marker at different SCUs, the start of the synchronization window must be properly calculated. In Sec. 5.2.1.3, the calculation of the synchronization window will be explained.

For both the phase shift and frequency beating method, the calculation is based on the predicted phase advance. The phase advance prediction module extrapolates the rf phase $\psi^{SIS100}_{h=1}$ for SIS100 rf h=1 (157kHz) signal and $\psi^{SIS18}_{h=1/5}$ for SIS18 rf h=1/5 (157kHz) signal at t_{ψ}. The more time is spent for the phase advance prediction, the

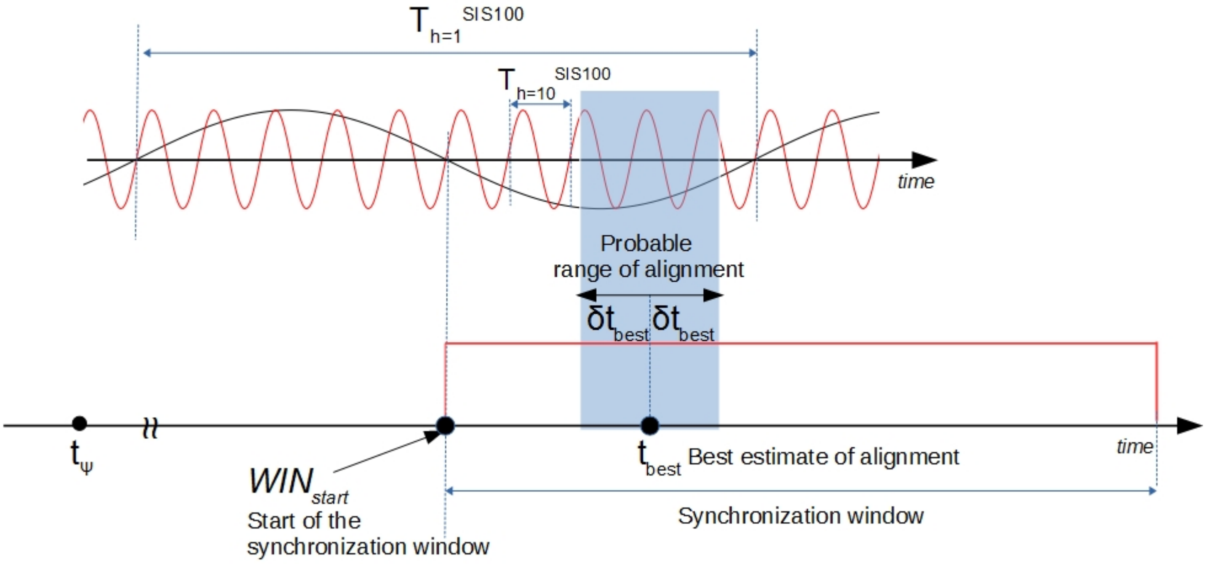

Abbildung 5.9: The illustration of the best estimate of alignment, the probable range of alignment and the synchronization window

better the predicted phase will be. More details about the phase advance measurement and phase advance prediction modules, please see Tibo's thesis. Fig. 5.10 illustrates some basic definition of symbols for the calculation. $\phi_{h=2}^{SIS18}$and $\phi_{h=10}^{SIS100}$ are individual rf phase of SIS18 and SIS100 rf refefrence signals at t_ψ. The relationship between $\phi_{h=2}^{SIS18}$, $\phi_{h=10}^{SIS100}$ and $\psi_{h=1/5}^{SIS18}$, $\psi_{h=1}^{SIS100}$ are given by eq. 5.18 and eq. 5.19.

$$\phi_{h=2}^{SIS18} = \frac{\frac{\psi_{h=1/5}^{SIS18}}{360°} \times T_{h=1/5}^{SIS18} \mod T_{h=2}^{SIS18}}{T_{h=2}^{SIS18}} \times 360° \tag{5.18}$$

$$\phi_{h=10}^{SIS100} = \frac{\frac{\psi_{h=1}^{SIS100}}{360°} \times T_{h=1}^{SIS100} \mod T_{h=10}^{SIS100}}{T_{h=10}^{SIS100}} \times 360° \tag{5.19}$$

substituting $T_{h=2}^{SIS18} \times 10 = T_{h=1/5}^{SIS18}$, $T_{h=10}^{SIS100} \times 10 = T_{h=1}^{SIS100}$ into eq.5.18 and eq.5.19 yields

$$\phi_{h=2}^{SIS18} = \frac{\frac{\psi_{h=1/5}^{SIS18} \times 10}{360°} \times T_{h=2}^{SIS18} \mod T_{h=2}^{SIS18}}{T_{h=2}^{SIS18}} \times 360° \tag{5.20}$$

$$\phi_{h=10}^{SIS100} = \frac{\frac{\psi_{h=1}^{SIS100} \times 10}{360°} \times T_{h=10}^{SIS100} \mod T_{h=10}^{SIS100}}{T_{h=10}^{SIS100}} \times 360° \tag{5.21}$$

Here we explain the inevitable uncertainty of the phase advance prediction and rf frequency modulation.

- Uncertainty of the predicted phase advance

  If the phase prediction time is 500us, the uncertainty of the predicted phase advance $\delta\delta t_\psi$ is 100ps. We calculate the uncertainty of the predicted phase advance, $\delta\psi_{h=1/5}^{SIS18}$ and $\psi_{h=1}^{SIS100}$, from the time to phase domain.

$$\delta t_\psi = 100ps \tag{5.22}$$

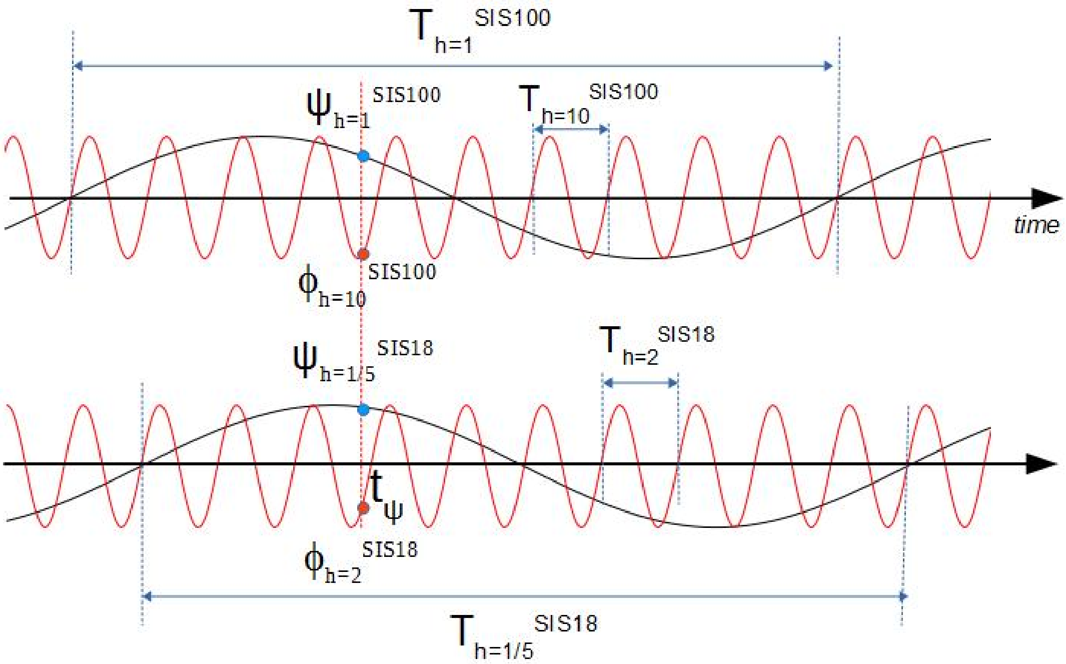

Abbildung 5.10: The illustration of symbols for the calculation

$$\delta\psi_{h=1/5}^{SIS18} = \delta\psi_{h=1}^{SIS100} = \frac{100ps}{1/157kHz} \times 360° \approx 0.006° \tag{5.23}$$

Based on the eq. 5.23, eq. 5.20 and eq. 5.21, the uncertainty of the phase at the rf reference frequencies of SIS18 and SIS100, $\delta\phi_{h=2}^{SIS18}$ and $\delta\phi_{h=10}^{SIS100}$, is calculated.

$$\delta\phi_{h=2}^{SIS18} = \sqrt{(\frac{\partial\phi_{h=2}^{SIS18}}{\partial\psi_{h=2}^{SIS18}}\delta\psi_{h=2}^{SIS18})^2} = \sqrt{(10 \times \delta\psi_{h=2}^{SIS18})^2} = 0.06° \tag{5.24}$$

$$\delta\phi_{h=10}^{SIS100} = \sqrt{(\frac{\partial\phi_{h=10}^{SIS100}}{\partial\psi_{h=1}^{SIS100}}\delta\psi_{h=10}^{SIS100})^2} = \sqrt{(10 \times \delta\psi_{h=10}^{SIS100})^2} = 0.06° \tag{5.25}$$

- Uncertainty of the rf frequency modulation

  For the rf frequency modulation, the jitter is 0.2° at 5.4MHz. We calculate the jitter in time domain, see eq. 5.26.

$$\delta\Delta f_{(t)} = \frac{0.2°}{360°} \times \frac{1}{5.4MHz} = 100ps \tag{5.26}$$

5.2.1.1 The best estimate of alignment and the probable range of alignment for the phase shift method

Different relation between $\phi_{h=2}^{SIS18}$ and $\phi_{h=10}^{SIS100}$ has different required phase adjustment for SIS18. Fig. 5.11 illustrates all scenarios of their relation and the required phase

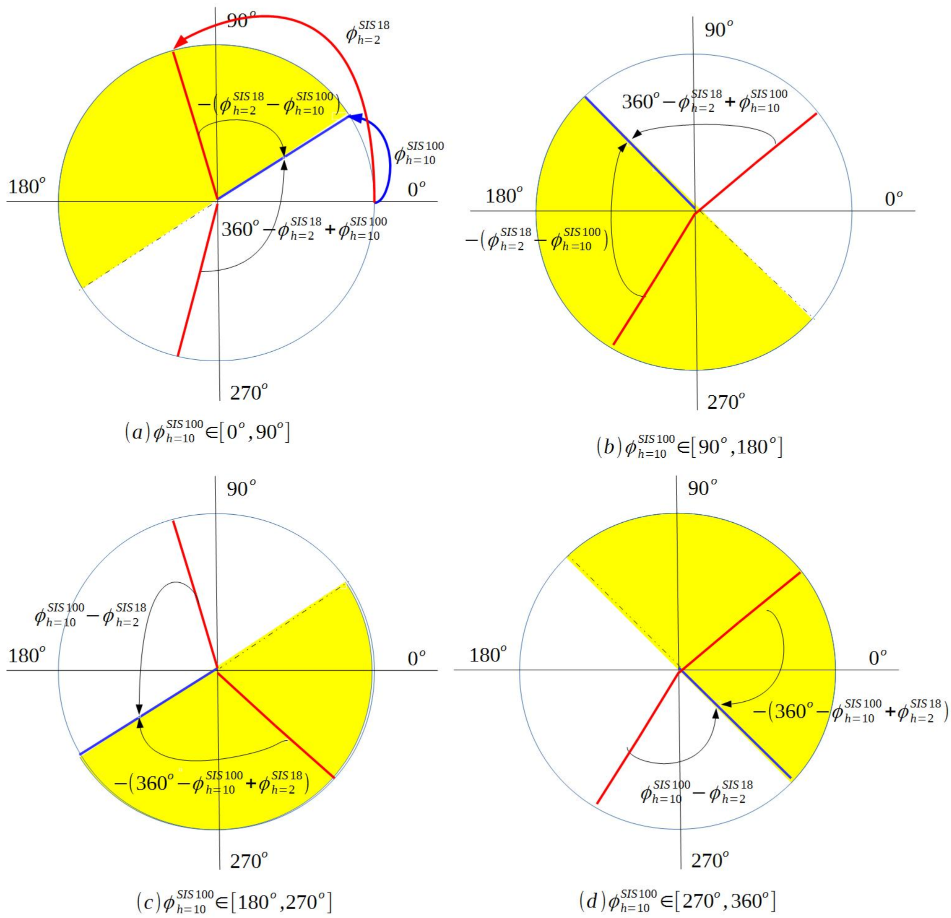

Abbildung 5.11: Scenarios for the phase shift method

adjustment for each scenario. We would like to introduce a phase shift of up to ±180°. The blue and red line represents the phase of SIS100 and SIS18 RF Reference Signal. The clockwise arrow from the SIS18 to SIS100 rf phase represents the negative phase adjustment for SIS18 and the anticlockwise represents the positive phase adjustment. The required phase adjustment of SIS18 is denoted by $\Delta\phi_{shift}$.

- Scenario (a): $\phi_{h=10}^{SIS100} \in [0, 90°)$, see Fig. 5.12 (a).

  - $\phi_{h=10}^{SIS100} < \phi_{h=2}^{SIS18} < \phi_{h=10}^{SIS100} + 180°$, which denotes by the yellow semicircle in Fig. 5.12 (a). The phase adjustment is

$$\Delta\phi_{shift} = -(\phi_{h=2}^{SIS18} - \phi_{h=10}^{SIS100}) \tag{5.27}$$

  - $\phi_{h=2}^{SIS18} < \phi_{h=10}^{SIS100}$ or $\phi_{h=2}^{SIS18} > \phi_{h=10}^{SIS100} + 180°$, which denotes by the white semicircle in Fig. 5.12 (a). The phase adjustment is

$$\Delta\phi_{shift} = 360° - \phi_{h=2}^{SIS18} + \phi_{h=10}^{SIS100} \tag{5.28}$$

- Scenario (b): $\phi_{h=10}^{SIS100} \in [90, 180°)$, see Fig. 5.12 (b).

  - $\phi_{h=10}^{SIS100} < \phi_{h=2}^{SIS18} < \phi_{h=10}^{SIS100} + 180°$, which denotes by the yellow semicircle in Fig. 5.12 (b). The phase adjustment is

$$\Delta\phi_{shift} = -(\phi_{h=2}^{SIS18} - \phi_{h=10}^{SIS100}) \tag{5.29}$$

- $\phi_{h=2}^{SIS18} < \phi_{h=10}^{SIS100}$ or $\phi_{h=2}^{SIS18} > \phi_{h=10}^{SIS100} + 180°$, which denotes by the white semicircle in Fig. 5.12 (b). The phase adjustment is

$$\Delta\phi_{shift} = 360° - \phi_{h=2}^{SIS18} + \phi_{h=10}^{SIS100} \tag{5.30}$$

- Scenario (c): $\phi_{h=10}^{SIS100} \in [180, 270°)$, see Fig. 5.12 (c). The phase adjustment is

- $\phi_{h=2}^{SIS18} > \phi_{h=10}^{SIS100}$ or $\phi_{h=2}^{SIS18} < \phi_{h=10}^{SIS100} + 180° - 360°$, which denotes by the yellow semicircle in Fig. 5.12 (c). The phase adjustment is

$$\Delta\phi_{shift} = -(360° - \phi_{h=10}^{SIS100} + \phi_{h=2}^{SIS18}) \tag{5.31}$$

- $\phi_{h=10}^{SIS100} - 180° < \phi_{h=2}^{SIS18} < \phi_{h=10}^{SIS100}$, which denotes by the white semicircle in Fig. 5.12 (c). The phase adjustment is

$$\Delta\phi_{shift} = \phi_{h=10}^{SIS100} - \phi_{h=2}^{SIS18} \tag{5.32}$$

- Scenario (d): $\phi_{h=10}^{SIS100} \in [270, 360°)$, see Fig. 5.12 (d).

- $\phi_{h=10}^{SIS100} - 180° < \phi_{h=2}^{SIS18} < \phi_{h=10}^{SIS100}$, which denotes by the yellow semicircle in Fig. 5.12 (d). The phase adjustment is

$$\Delta\phi_{shift} = \phi_{h=10}^{SIS100} - \phi_{h=2}^{SIS18} \tag{5.33}$$

- $\phi_{h=2}^{SIS18} > \phi_{h=10}^{SIS100}$ or $\phi_{h=2}^{SIS18} < \phi_{h=10}^{SIS100} + 180° - 360°$, which denotes by the white semicircle in Fig. 5.12 (d).

$$\Delta\phi_{shift} = -(360° - \phi_{h=10}^{SIS100} + \phi_{h=2}^{SIS18}) \tag{5.34}$$

The phase adjustment is achieved by the phase shift method within the upper bound time, $T_{phase\_shift}^{upper\_bound}$. For the U^{28+} B2B transfer from SIS18 to SIS100, we assume that $T_{phase\_shift}^{upper\_bound}$ equals to 7ms, which means that the phase shift $\Delta\phi_{shift}$ is achieved within 7ms. So the best estimate of alignment is expressed by

$$t_{best} = t_{\psi} + T_{phase\_shift}^{upper\_bound} \tag{5.35}$$

The uncertainty in the phase prediction δt_{ψ} is 100ps, see eq. 5.22. The phase shift uncertainy $\delta\Delta\phi_{phase}$ is casued by the rf frequency modulation, whose jitter is 100ps, see eq. 5.26. The phase shift uncertainy equals to the uncertainty in the phase shift upper bound time, $\delta T_{phase_shift}^{upper_bound} = 100$ps. Both cause an uncertainty in the best estimate of alignment t_{best}.

$$\begin{aligned}\delta t_{best} &= \sqrt{(\frac{\partial t_{best}}{\partial t_{\psi}}\delta t_{\psi})^2 + (\frac{\partial t_{best}}{\partial T_{phase\_shift}^{upper\_bound}}\delta T_{phase\_shift}^{upper\_bound})^2} \\ &= \sqrt{(\delta t_{\psi})^2 + (T_{phase\_shift}^{upper\_bound})^2} = \sqrt{100ps^2 + 100ps^2} \approx 140ps\end{aligned} \tag{5.36}$$

The uncertainty of the alignment for the phase shift method is about 140ps. So the proper range of alignment is [t_{best}-140ps, t_{best}+140ps] for U^{28+} B2B transfer from SIS18 to SIS100.

5.2.1.2 The best estimate of alignment and the probable range of alignment for the frequency beating method

Fig. 5.12 illustrates two scenarios for the frequency beating method. With the frequency beating method, SIS18 can only achieve positive phase adjustment, which is denoted by $\Delta\phi_{adjustment}$. E.q. 5.37 shows the best estimate of alignment for the phase adjustment of $\Delta\phi_{adjustment}$.

$$t_{best} = t_\psi + \frac{\Delta\phi_{adjustment}}{360^\circ \times \Delta f} \tag{5.37}$$

where Δf is the beating frequency.

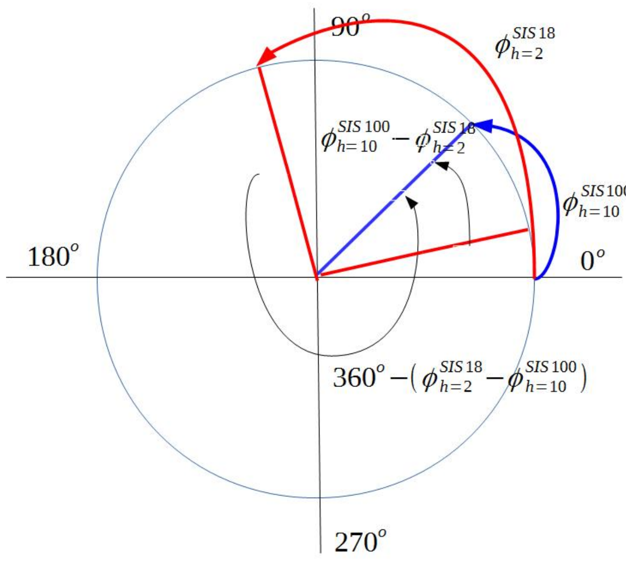

Abbildung 5.12: Two scenarios for the frequency beating method

According to the relation between $\phi_{h=2}^{SIS18}$ and $\phi_{h=10}^{SIS100}$, there are two scenarios, see Fig. 5.12.

- Scenario (a): $\phi_{h=2}^{SIS18} < \phi_{h=10}^{SIS100}$

$$\Delta\phi_{adjustment} = \phi_{h=10}^{SIS100} - \phi_{h=2}^{SIS18} \tag{5.38}$$

Replacing $\Delta\phi_{adjustment}$ in eq. 5.37 with eq. 5.38, we have

$$t_{best} = t_\psi + \frac{\phi_{h=10}^{SIS100} - \phi_{h=2}^{SIS18}}{360^\circ \times \Delta f} \tag{5.39}$$

- Scenario (b): $\phi_{h=2}^{SIS18} \geq \phi_{h=10}^{SIS100}$

$$\Delta\phi_{adjustment} = 360^\circ - (\phi_{h=2}^{SIS18} - \phi_{h=10}^{SIS100}) \tag{5.40}$$

Replacing $\Delta\phi_{adjustment}$ in eq. 5.37 with eq. 5.40, we have

$$t_{best} = t_\psi + \frac{360^\circ - (\phi_{h=2}^{SIS18} - \phi_{h=10}^{SIS100})}{360^\circ \times \Delta f} \tag{5.41}$$

Based on these two scenarios, we could deduce the formula for the best estimate of alignment.

$$t_{best} = t_{\psi} + \frac{\Delta n \times 360° - (\phi^{SIS18}_{h=2} - \phi^{SIS100}_{h=10})}{360° \times \Delta f} \tag{5.42}$$

where $\triangle n$ equals 0 when $\phi^{SIS18}_{h=2} < \phi^{SIS100}_{h=10}$ and equals 1 when $\phi^{SIS18}_{h=2} \geq \phi^{SIS100}_{h=10}$.

The uncertainty of the alignment is the result of the propagation of uncertainties of the phase prediction and rf frequency detune, see eq. 5.43. Because the rf frequency detune has the long term stability, $\int \delta\Delta f$=0, the uncertainty caused by rf frequency detune is 0. The uncertainty of the phase prediction $\phi^{SIS18}_{h=2}$ and $\phi^{SIS100}_{h=10}$ is 0.06°, see eq. 5.24 and eq. 5.25. Δf is 200Hz. The maximum $\Delta n \times 2\pi - (\phi^{SIS18}_{h=2} - \phi^{SIS100}_{h=10})$ is 2π.

$$\begin{aligned}
\delta t_{best} &= \sqrt{(\frac{\partial t_{best}}{\partial \phi^{SIS18}_{h=2}}\delta\phi^{SIS18}_{h=2})^2 + (\frac{\partial t_{best}}{\partial \phi^{SIS100}_{h=10}}\delta\phi^{SIS100}_{h=10})^2 + (\frac{\partial t_{best}}{\partial \Delta f}\delta\Delta f)^2} \\
&= \sqrt{(\frac{-1}{2\pi \times \Delta f}\delta\phi^{SIS18}_{h=2})^2 + (\frac{1}{2\pi \times \Delta f}\delta\phi^{SIS100}_{h=10})^2 + (-\frac{\Delta n \times 2\pi - (\phi^{SIS18}_{h=2} - \phi^{SIS100}_{h=10})}{2\pi \times \Delta f^2}\delta\Delta f)^2} \\
&\leq \sqrt{(\frac{-1}{2\pi \times 200}0.06°)^2 + (\frac{1}{2\pi \times 200}0.06°)^2 + 0} \\
&\approx 1.178us
\end{aligned} \tag{5.43}$$

From eq. 5.43 we could get the uncertainty of the alignment is 1.178us, so the probable range of alignment is $[t_{best}$–$1.178us, t_{best} + 1.178us]$.

5.2.1.3 Calculation the synchronization window and its accuracy

In the last section, we get the probable range of alignment, within which the two rf frequency signals will be fine aligned with each other. The synchronization window is used to select the revolution frequency marker for the extraction and injection kicker firing, which is closest to the probable range of alignment, See Fig. 5.13. For the selection, the length of the synchronization window must be a least one SIS100 revolution period. The best estimate of the start of the synchronization window is exactly half revolution period before the selected revolution frequency marker. The blue and orange rectangles represent two scenarios of the probable range of alignment. In Fig. 5.13, the 2nd revolution frequency marker is the closest one to the probable range of alignment. The best estimate of the start of the synchronziation window aligns with the negative zero crossing point of the revolution marker signal.

For SIS100, the rf phase of the revolution frequency is $\psi^{SIS100}_{h=1}$ at t_{ψ}. We could calculate the rf phase $\psi_{s\_alignment}$ at the start of the probable rang of alignment, t_{best}-δt_{best}.

$$\psi_{s\_alignment} = \frac{(t_{best} - \delta t_{best} - t_{\psi} - \frac{360° - \psi^{SIS100}_{h=1}}{360°} \times T^{SIS100}_{h=1}) \mod T^{SIS100}_{h=1}}{T^{SIS100}_{h=1}} \times 360° \tag{5.44}$$

For the calculation of the best estimate of the start of the synchronization window, there are two scenarios. $\Delta t_{win\_correct}$ is the time correction for the start of the probable range of alignment to the best estimate of the start of the synchronization window, see Fig. 5.13.

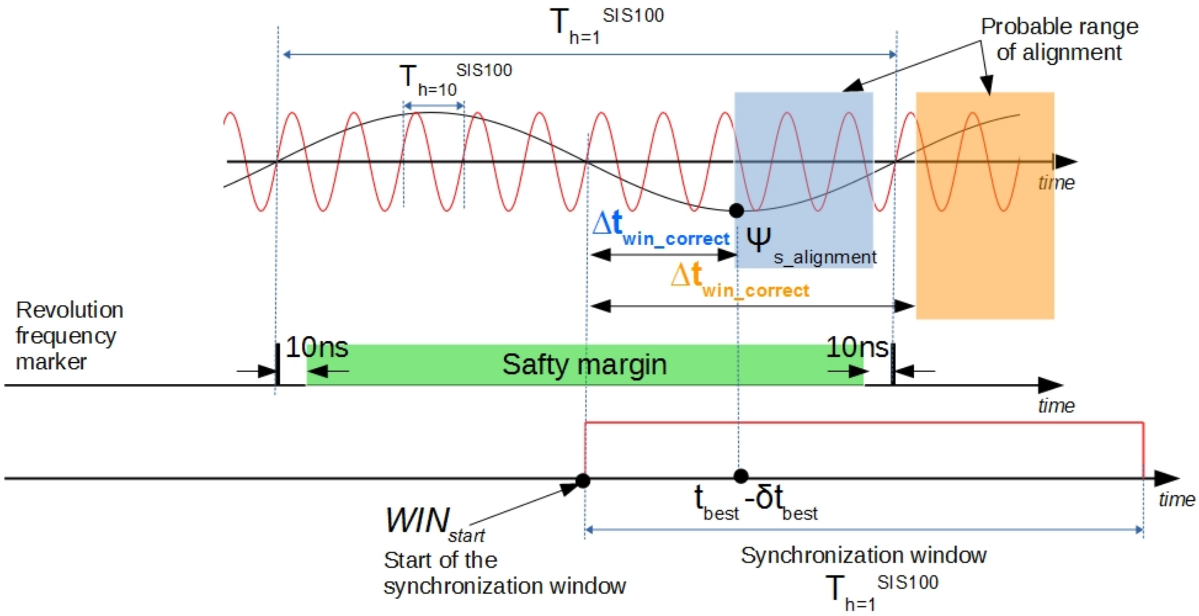

Abbildung 5.13: The illustration of the synchronization window and its accuracy

- $\psi_{s\_alignment} \in [0°, 180°)$, the orange rectangle in Fig. 5.13

$$\Delta t_{win\_correct} = \frac{\psi_{s\_alignment}}{360°} \times T_{h=1}^{SIS100} + \frac{T_{h=1}^{SIS100}}{2} \tag{5.45}$$

$$WIN_{start} = t_{best} - \delta t_{best} - \Delta t_{win\_correct} \tag{5.46}$$

- $\psi_{s\_alignment} \in [180°, 360°)$, the blue rectangle in Fig. 5.13

$$\Delta t_{win\_correct} = \frac{\psi_{s\_alignment} - 180°}{360°} \times T_{h=1}^{SIS100} \tag{5.47}$$

$$WIN_{start} = t_{best} - \delta t_{best} - \Delta t_{win\_correct} \tag{5.48}$$

The actual start of the synchronization window is impossible to be exactly at the best estimate of the start of the synchronization window because of the precision and trueness [?]. The precision is defined as the closeness of agreement between the actual start of the synchronization window of different SCUs and the trueness as the closeness of agreement between the average actual start of the synchronization window of different SCUs and the best estimation start of the synchronization window. The precision comes from the random error, e.g. IO port TTL signal rising osillation ???. The trueness is the systematic error, e.g. FPGA process time. The accuracy is defined as the closeness of agreement between the observed start and the best estimate of the start of the synchronization window, which is the sum of the precision and trueness. Because the B2B transfer system is used for all FAIR project, we must find the most stringent accuracy requirement. The shortest revolution period of the target machine is 433 ns, which comes from RIB transfer from CR to HESR. We keep 10ns as a forbidden range, which means that the actual start is not allowed 10 ns before and after the revolution frequency marker. The green region in

Fig. 5.13 represents the safty margin for the start of the synchronization window. So the accuracy of the start of the synchronization window is

$$Accuracy = \pm\frac{433 - 10 \times 2}{2} \approx \pm 200\,\mathrm{ns} \tag{5.49}$$

5.2.2 Measurement of the WR network for the B2B transfer

GMT system implements the tree WR network topology. The WR network measurement is achieved by the Xena traffic generator, which offers a new class of professional Layer 2-3 Gigabit Ethernet test platform. It is used to measure the frame loss rate[1], latency[2] and jitter[3] for the WR network. For the measurement, Xena traffic generator sends the traffic streams with a unique stream ID for identifying latency, jitter and packet loss. The WR network for FAIR has the following traffic.

- DM Broadcast

  DM forwards broadcast timing frames[4] with 110 bytes ethernet frame length downwards to all FECs. The average bandwidth for the DM broadcast is 100 Mbit/s. The burst[5] speed is 12 packets per 100 µs.

- DM Unicast

  DM sends 10Mbit/s unicast timing frames with 110 bytes ethernet frame length to some specified FECs at the burst speed of 3 packets per 300 µs.

- B2B Unicast

  The source B2B SCU sends the timing frames with 110 bytes ethernet frame length upwards to the DM. For the B2B transfer upper bound time 10 ms of each supercycle, 2 unicast timing frames are send to the DM. The maximum repetition frequency is of the U^{28+} supercycle, 2.82 Hz. For the estimation of the upper bound bandwidth, we use 3Hz/s as the maximum repetition frequency. So the bandwidth is $3\,\mathrm{Hz/s} \times 2\,\mathrm{packets/supercycle} \times 110\,\mathrm{byte} \times 8\,\mathrm{bit} \approx 5.5\,\mathrm{kbit/s}$.

- B2B Broadcast

  Maximum 10 B2B broadcast timing frames with 110 ethernet frame length are sent within 10 ms. So the bandwidth is $3\,\mathrm{Hz/s} \times 10\,\mathrm{packets/supercycle} \times 110\,\mathrm{byte} \times 8\,\mathrm{bit} \approx 26.5\,\mathrm{kbit/s}$.

[1] The ratio of the number of the lost frames to the number of the theoretic received frames of a tested port.

[2] The time interval between the time of Xena port receiving frame and the time of another Xena port sending frame.

[3] The absolute value of the difference between the latency of two consecutive received frames belonging to the same stream from one Xena port to another Xena port. http://www.xenanetworks.com/wp-content/uploads/Measuring_Frame_latency_Variation.pdf

[4] https://www-acc.gsi.de/wiki/Timing/TimingSystemEvent

[5] A group of consecutive frames with shorter interframe gaps than frames arriving before or after the burst of frames.

- Management Traffic

  The average bandwidth for the management traffic is 10 Mbit/s. It broadcasts packets with random ethernet frame length from 64 bytes to 1518 bytes.

The requirements for the B2B Broadcast and Unicast traffic are summarized in Tab. 5.1.

Tabelle 5.1: The B2B transfer requirements for the WR network

	Frame Loss Rate	Upper bound latency of WR network	Upper bound latency per WR switch layer
B2B Broadcast	10^{-12}	500 µs	30 µs
B2B Unicast	10^{-12}	500 µs	30 µs

A Virtual Local Area Network (VLAN) is a group of FECs in the WR network that is logically segmented by function or application, without regard to the physical locations of the FECs. For the WR network for FAIR, three VLANs with different priorities are applied according to the importance of the traffic.

5.2.2.1 WR network test setup

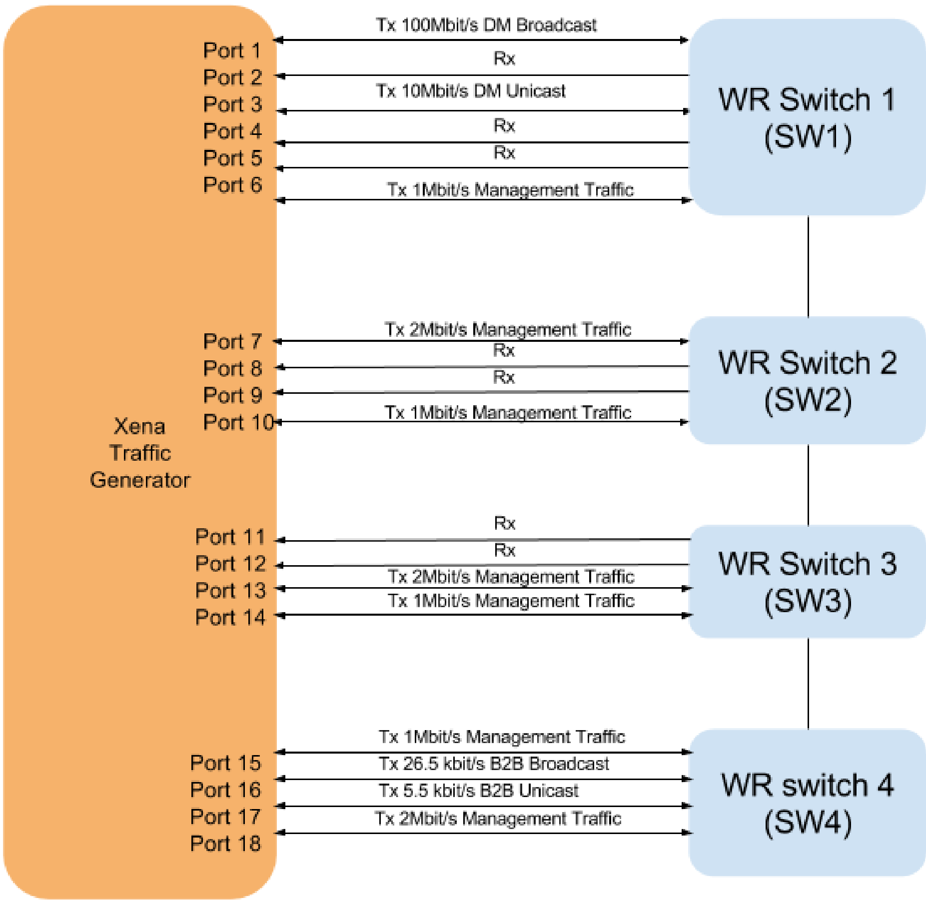

Abbildung 5.14: The WR network test setup

Based on the mentioned traffic, the measurement setup is built, see Fig. 5.14. Four WR switches are connected to the port 1 to 18 of the Xena traffic generator. All ports of four WR switches are assigned to three VLANs, VLAN 5, VLAN 6 and VLAN 7. Tab. 5.2 shows the bandwidth, VLAN, VLAN priority and usage of the traffic of each Xena port in details.

5.2.2.2 Frame loss rate test result for B2B frames

The frame loss rate of the stream from port 17 to port 1 is measured for the B2B Unicast frames. The frame loss rate of the stream from port 16 to other ports is measured for the B2B Broadcast frame. Fig. 5.15 shows the test result for both traffics. For the B2B Broadcast frames, the frame loss rate of each port is 0 %. For the B2B Unicast frames, the frame loss rate of port 1 is 0 %. So there is no B2B frame loss of the test WR network.

5.2.2.3 Latency and jitter test result for B2B frames

The latency and jitter of the stream from port 16 to other ports are measured.

Tabelle 5.2: The traffic of Xena ports

Switch	Xena Port	Traffic	VLAN	Priority	Usage
WR switch 1	Port 1	100 Mbit/s 110bytes	7	7	DM Broadcast
WR switch 1	Port 2	Rx traffic			
WR switch 1	Port 3	10 Mbit/s 110bytes	7	7	DM Unicast
WR switch 1	Port 4	Rx traffic			
WR switch 1	Port 5	Rx traffic			
WR switch 1	Port 6	1 Mbit/s 64 - 1518 bytes	5	5	Management Broadcast
WR switch 2	Port 7	2 Mbit/s 64 - 1518 bytes	5	5	Management Broadcast
WR switch 2	Port 8	Rx traffic			
WR switch 2	Port 9	Rx traffic			
WR switch 2	Port 10	1 Mbit/s 64 - 1518 bytes	5	5	Management Broadcast
WR switch 3	Port 11	Rx traffic			
WR switch 3	Port 12	Rx traffic			
WR switch 3	Port 13	2 Mbit/s 64 - 1518 bytes	5	5	Management Broadcast
WR switch 3	Port 14	1 Mbit/s 64 - 1518 bytes	5	5	Management Broadcast
WR switch 4	Port 15	1 Mbit/s 64 - 1518 bytes	5	5	Management Broadcast
WR switch 4	Port 16	26.5 kbit/s 110bytes	6	6	B2B Broadcast
WR switch 4	Port 17	5.5 kbit/s 110bytes	7	7	B2B Unicast
WR switch 4	Port 18	2 Mbit/s 64 - 1518 bytes	5	5	Management Broadcast

- Latency and jitter for B2B Broadcast frames

  - Average Latency and jitter

    Fig. 5.16 shows the test result for the average latency and jitter for the

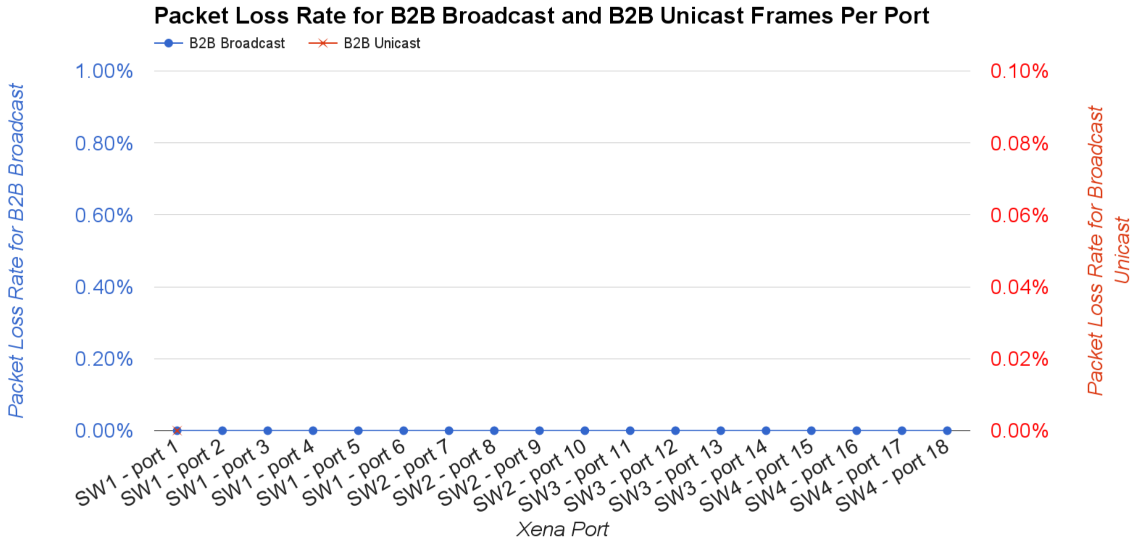

Abbildung 5.15: The frame loss rate for B2B Broadcast and B2B Unicast frames

B2B Broadcast frames. The average latency of the stream going through the WR switch 4 is approximate 6 µs. The average latency of the stream going through the WR switch 4 and 3 is approximate 8 µs. The average latency of the stream going through the WR switch 4, 3 and 2 is approximate 11 µs. The average latency of the stream going through the WR switch 4, 3, 2 and 1 is approximate 14 µs. The average jitter of each port is 0 ns. From the viewpoint of the average jitter and latency, they meet the requirements of the B2B transfer.

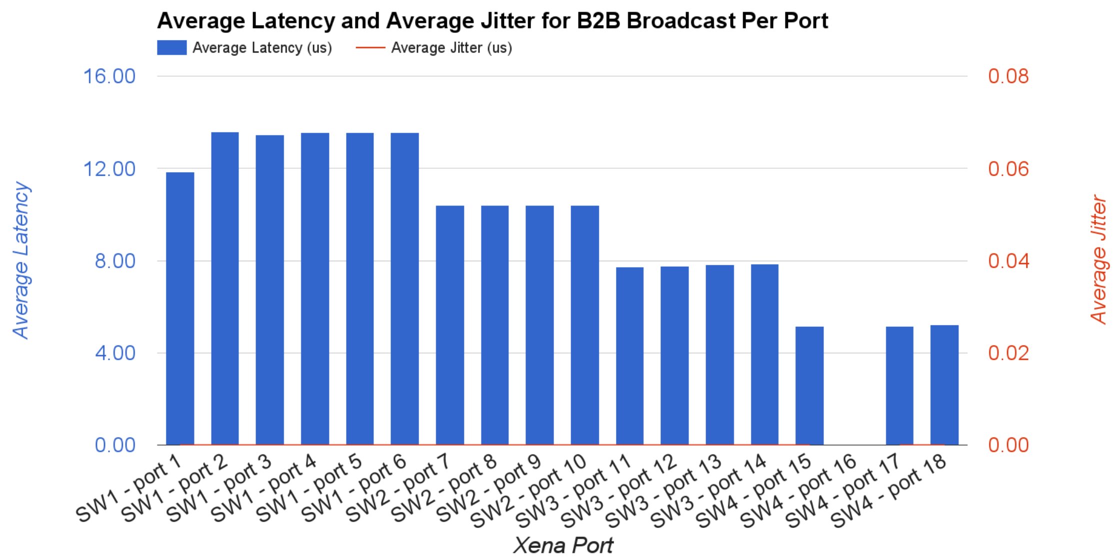

Abbildung 5.16: The average latency and jitter for B2B Broadcast frames

- Maximum Latency and jitter

Fig. 5.17 shows the test result for the maximum latency and jitter for the B2B Broadcast frames. The maximum latency and jitter of the stream going through the WR switch 4 is approximate 28 µs and 25 µs. The maximum latency and jitter of the stream going through the WR switch 4 and 3 is approximate 34 µs and 25 µs. The maximum latency and jitter of the stream going through the WR switch 4, 3 and 2 is approximate 37 µs and 27 µs. The maximum latency and jitter of the stream going through the WR switch 4, 3, 2 and 1 is approximate 41 µs and 30 µs.

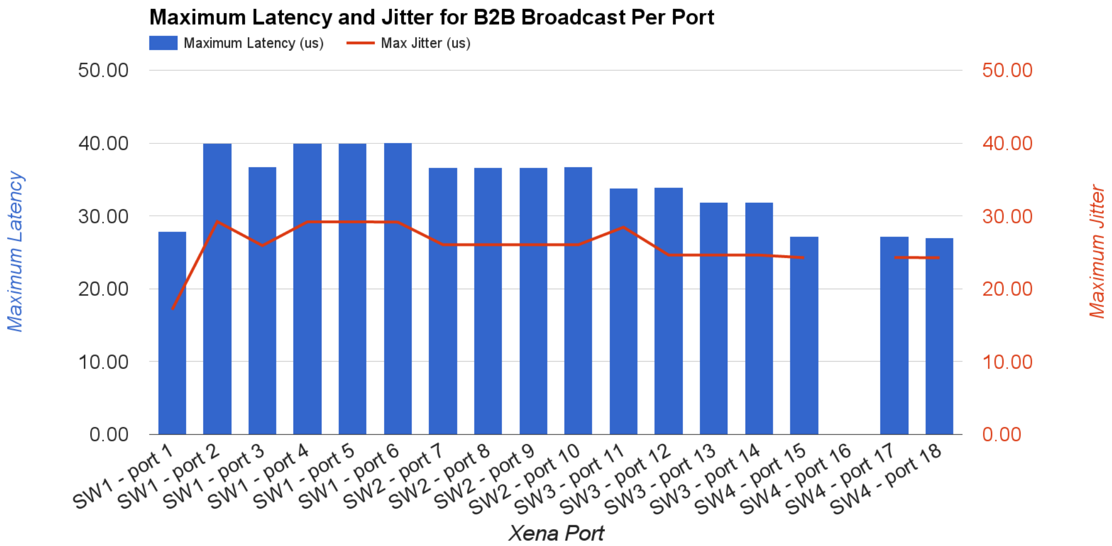

Abbildung 5.17: The maximum latency and jitter for B2B Broadcast frames

- Latency and jitter for B2B Unicast frames

  For the B2B unicast frames, the latency and jitter of the stream from port 16 to port 1 are measured.

  - Average Latency and jitter

    For the B2B Unicast frames, 4 WR switch network has approximate 11 µs average latency and 0 µs average jitter.

  - Maximum Latency and jitter

    For the B2B unicast frames, 4 WR switch network has approximate 23 µs maximum latency and 13 µs maximum jitter.

More test results, please see the document ——————-

5.2.2.4 Result and conclusion

Tab. 5.3 shows the result of the test. The frame loss rate and latency meet the requirements of the B2B Broadcast and B2B Unicast traffic.

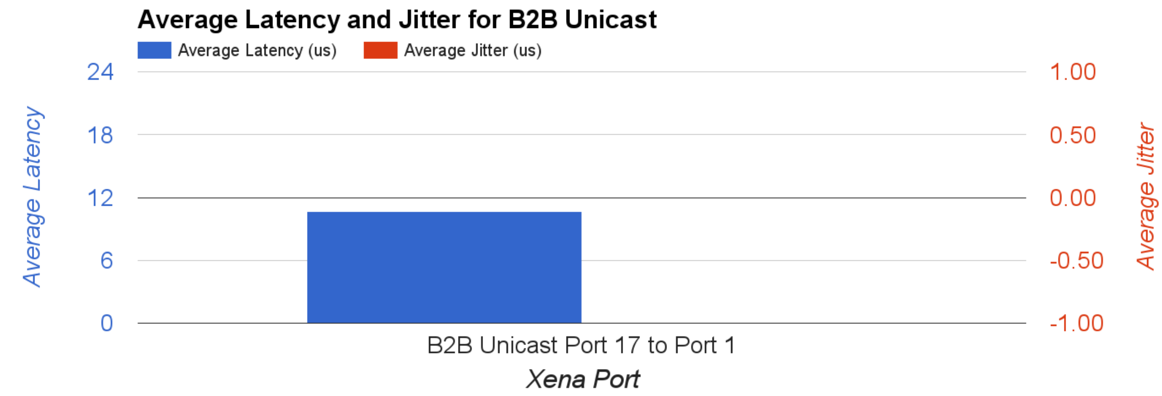

Abbildung 5.18: The average latency and jitter for B2B Unicast frames

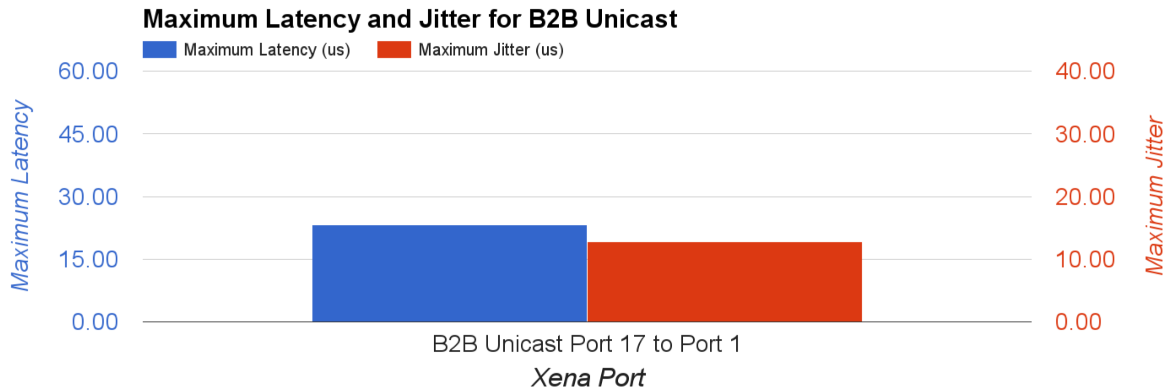

Abbildung 5.19: The maximum latency and jitter for B2B Unicast frames

Tabelle 5.3: The result of the test

	Frame Loss Rate	Average Latency	Maximum Latency	Average Jitter	Maximum Jitter
B2B Broadcast	0 %	6 µs/switch	28 µs/switch	0 µs/switch	25 µs/switch
B2B Unicast	0 %	11 µs/4switch 3 µs/switch	23 µs/4switch 6 µs/switch	0 µs/4switch 0 µs/4switch	13 µs/4switch 4 µs/switch

For the B2B transfer system, the upper bound latency of the frames in the B2B Broadcast and B2B Unicast traffic is 500 µs, see Sec.5.2.2. The latency of the WR network is decided by the layers of WR switches and the length of the optical fiber. The latency of the optical fiber is about 204 m/µs and the longest distance in the FAIR campus is around 2 km, so the latency of a 2 km optical fiber is about 10 µs. The layers of WR switches plays a more important role in the latency.

- B2B Broadcast

Here we canculate the layer of the WR switch between the B2B source SCU and B2B target SCU, between B2B source SCU and source trigger SCU and between B2B source SCU and target trigger SCU.

$$\frac{500\,\mu s - 10\,\mu s}{28\,\mu s/\text{switch}} \approx 17 \tag{5.50}$$

- B2B Unicast

  Here we canculate the layer of the WR switch between the B2B source SCU and DM.

$$\frac{500\,\mu s - 10\,\mu s}{6\,\mu s/\text{switch}} \approx 81 \tag{5.51}$$

5.3 Kicker systematic investigation for the B2B transfer system

The SIS18 extraction kicker consists of 9 kicker units. In the existing topology, 5 kicker units are installed in the 1st crate and the other 4 units are in the 2nd crate. The width of each kicker unit is 0.25m and the distance between two kicker units is 0.09m. The distance between two crates is 19.167m. SIS100 injection kicker consists of 6 kicker units, which are equally located. The width of each kicker unit is 0.22m and the distance between two units is 0.23m. For the B2B transfer, the rise time of SIS18 extraction kicker and SIS100 injection kicker unit are 90ns and 1/20 of the revolution period. The rise time of these kickers must fit within the bunch gap, 25% of rf reference period. The bunch gap is denoted by G. All the analysis in this section dose not consider the jitter of the kicker trigger signal. Here we are discussing about the following possibilities.

- For SIS18, whether the kicker units in the 2nd crate could be fired a fixed delay after the firing of the kicker units in the 1st crate for ion beams over the whole range of stable isotopes.
- For SIS100, whether the kicker units could be fired instantaneously.

5.3.1 SIS18 extraction kicker units

Here we take three ion beams, $H^{+}, U^{28} and U^{73+}$, to check the possibility, because the boundary ion species have the most stringent requirements. Fig. 5.20 shows three scenarios of the firing delay between two crates. Beam is firstly kicked by kicker units in the 1st crate and than kicked by the units in the 2nd crate to the transfer line. The yellow and red ellipse represents the position of the bunches, when the kicker units in the 1st and 2nd crate are fired. The number in the ellipse is used to tell different bunches. The head of the bunch is at the right side. The bunch 2 is firstly kicked. Here we assume that the kicker units in the same crate are triggered instantaneous. d denotes the distance between two crates. L denotes the distance from the leftmost to the rightmost kicker unit. D denotes the sum distance of d and the 2nd crate. d equals to 19.167 meter. L equals to 22.047m = d + 9×0.25$m + 7\times$ 0.09m. D equals to 20.437m = d + 4×0.25$m + 3\times$ 0.09m.

Fig. 5.20 (a) is the easiest scenario. The kicker units in the 1st crate are fired when the tail of the bunch 1 passes by the 1st crate completely. The kicker units in the 2nd crate are fired when the tail of the bunch 1 passes by the 2nd crate completely. The delay for the firing two crates in this scenario is D/βc.

Fig. 5.20 (b) shows the scenario of the maximum delay between the firing of two crates. The kicker units in the 1st crate are fired when the tail of the bunch 1 passes by the 1st crate completely. The kicker units in the 2nd crate are fired 90ns before the head of the bunch 2 passes by it. The delay equals to G+d/βc-90ns.

Fig. 5.20 (c) shows the scenario of the minimum delay. The kicker units in the 1st crate are fired 90ns before the head of the bunch 2 passes by it. The kicker units in the 2nd crate are fired when the bunch 1 passes by the 2nd crate. The delay is L/βc-G+90ns.

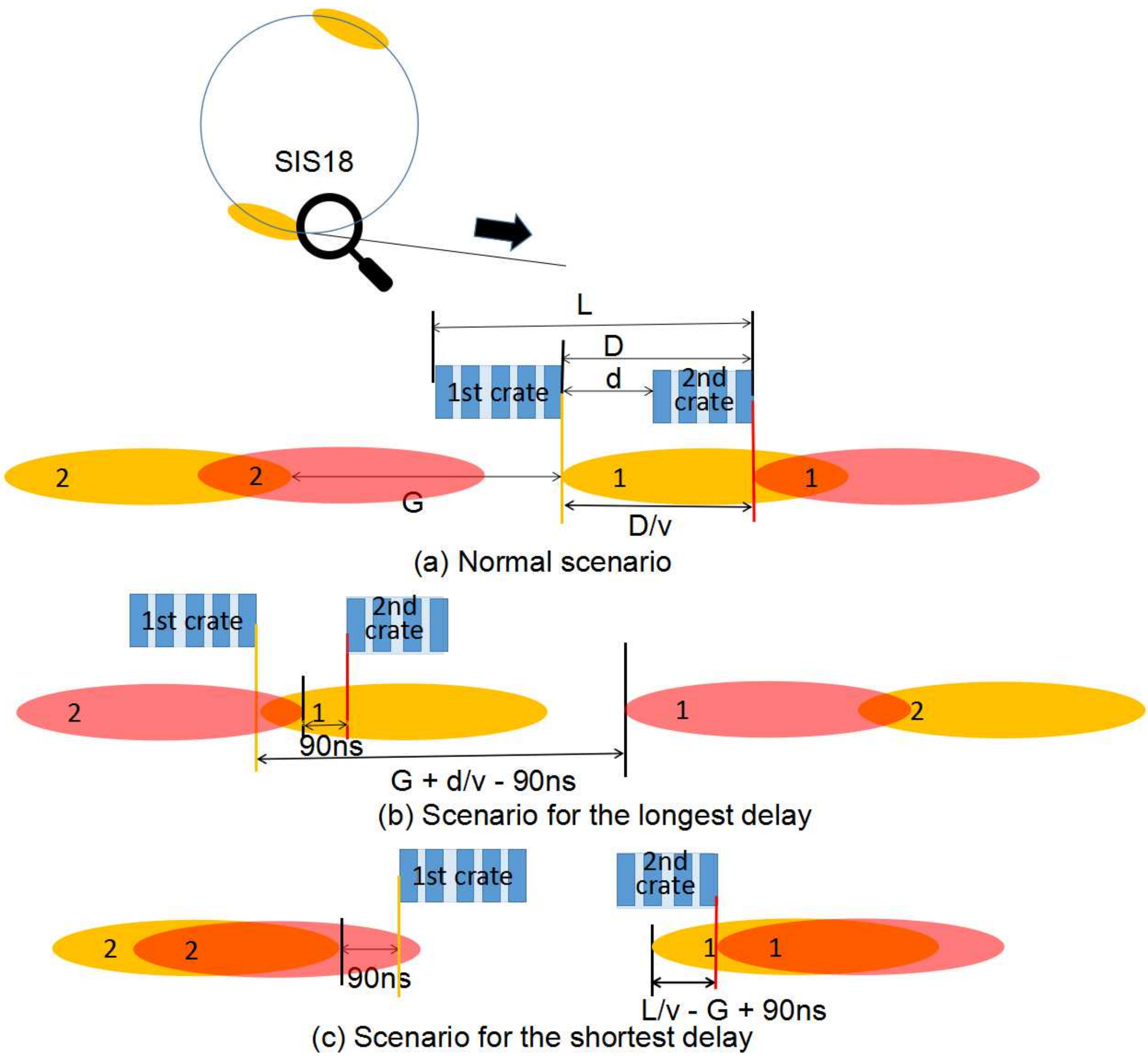

Abbildung 5.20: Three scenarios for the delay of SIS18 extraction kicker

Table 5.4 shows delay for three scenarios and related parameters. The fixed delay is determined primarily by the boundary delay range from $H^{+}, U^{28} and U^{73+}$ beams, the delay range for other heavy ion species beams must be contained in these boundary range. According to the result, a fixed delay is available for firing kicker units in two crate for different beams. e.g. 80ns.

Tabelle 5.4: The delay for firing two crates of SIS18 extraction kicker

Beam	β	time L/βc	bunch gap G	minimum delay L/βc-G+90ns	delay D/βc	maximum delay G+d/βc-90ns
H^+	0.982	75ns	184ns	0ns	69ns	163ns
U^{28}	0.568	130ns	159ns	61ns	120ns	189ns
U^{73+}	0.872	84ns	104ns	70ns	78ns	92ns

5.3.2 SIS100 injection kicker units

Two bunches from SIS18 will be continuously injected into one RF bucket after the other in SIS100. See Fig. 5.5. The yellow ellipse represents the circulating bunch in SIS100 and the red one represents the bunch to be injected. The head of the bunch is at the left side. The preparation of the SIS100 injection kicker must be done during the bunch gap and it must be established for at least one SIS18 revolution period. For the instantaneous firing, all kicker units are fired only if the tail of the circulating bunch passes the leftmost kicker unit. The kicker pass time is the time needed for the tail of a bunch to pass from the rightmost unit to the leftmost kicker unit. The rise time of the kicker unit is 1/20 of the revolution period. Therefor the preparation time is the sum of the kicker pass time and rise time. The distance from the rightmost to the leftmost kicker unit is 3.79m, 6 $\times 0.22m + 5 \times$0.23m. If the preparation time is shorter than bunch gap, all kicker units could be fired instantaneous. Table 5.5 shows the preparation time for $H^+, U^{28} and U^{73+}$ beams and their bunch gap. The preparation time is much shorter than the bunch gap. So the kicker units could be fired instantaneous.

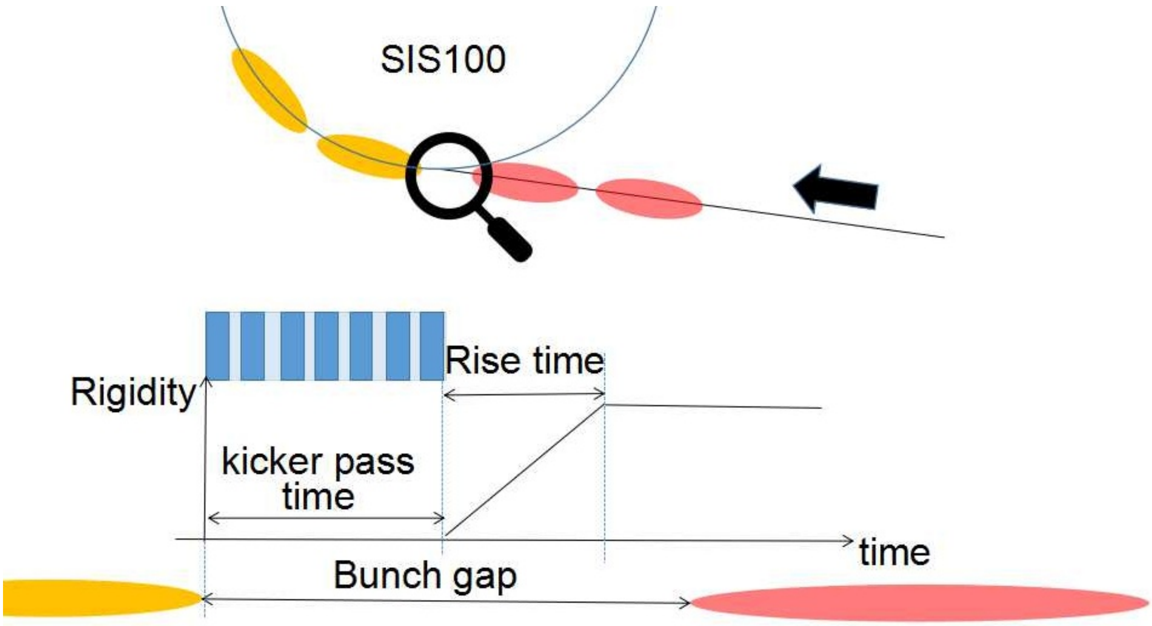

Abbildung 5.21: SIS100 injection kicker

Tabelle 5.5: The delay for firing SIS00 injection kicker

Beam	β	kicker pass time L/βc	Rise time $1/20\times T_{rev}^{SIS100}$	Preparation time L/βc+$1/20\times T_{rev}^{SIS100}$	bunch gap $2.25\times T_{rev}^{SIS100}$
H^+	0.982	3ns	184ns	187ns	828ns
U^{28}	0.568	22ns	318ns	333ns	1431ns
U^{73+}	0.872	15ns	207ns	222ns	932ns

5.4 Test setup for the data collection, merging and redistribution of the B2B transfer system

In this section, the test setup for the B2B transfer system is described, focusing only on the timing aspects.

5.4.1 Test functional requirement

The test setup achieves the following functional requirement.

- After receiving the B2B beginning event, both the B2B source and target SCUs collect predicted phase equivalent data locally. The equivalence is a timestamp for the zero crossing point of the simulated RF Reference Signal of SIS18 and SIS100.

- The B2B target SCU transfers the frame containing the timestamp to the B2B source SCU.

- After receving the data, the B2B source SCU calculates the synchronization window.

- The B2B source SCU sends the frame containing the beginning of the synchronization window to the WR network.

- After receving the frame, the trigger SCU produces TTL output indicating the start of the synchronization window.

5.4.2 Test setup

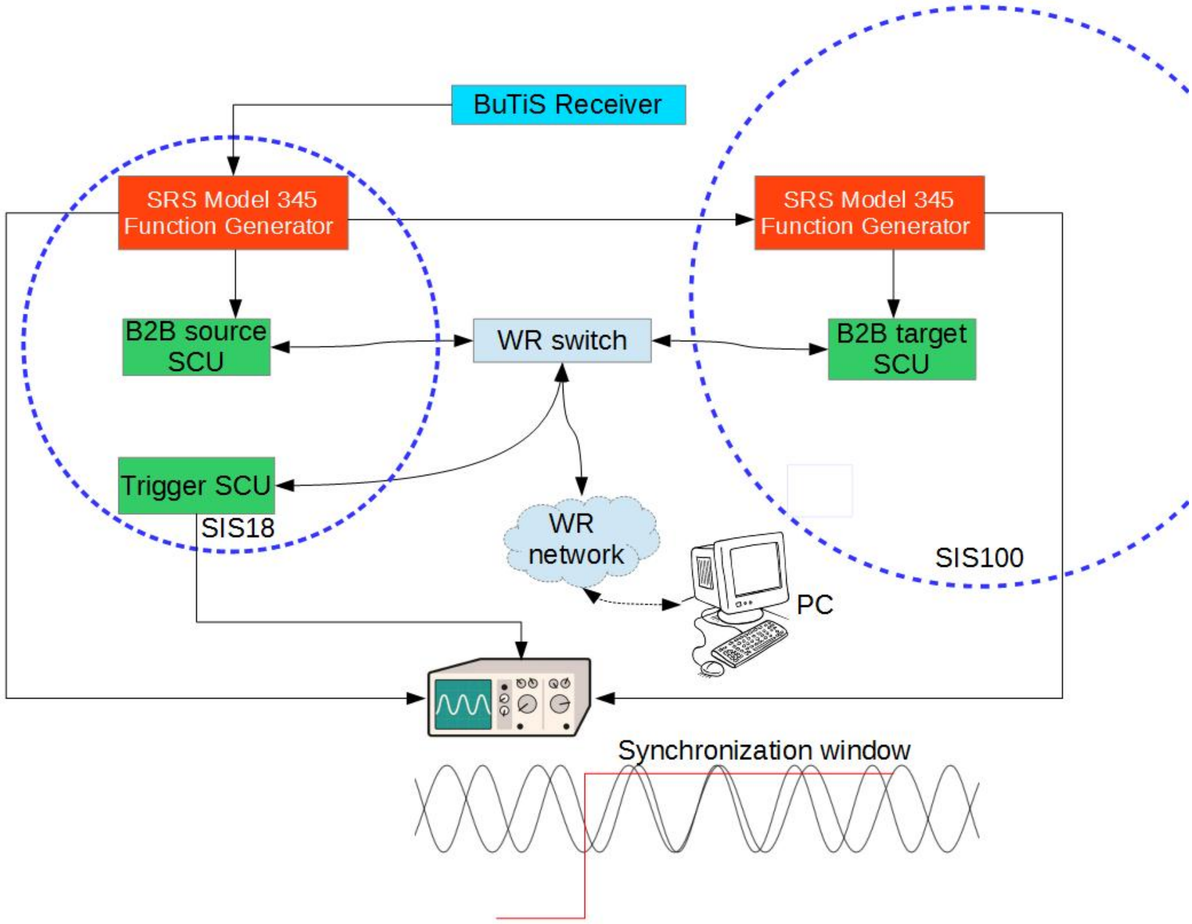

Abbildung 5.22: Schematic of the test setup

Fig. 5.22 shows the schematic of the test setup. In this test setup, two MODEL DS345 Synthesized Function Generators[6] are used, which are with the frequency accuracy of ±5 ppm of the selected frequency to simulate RF Reference Signals of SIS18 and SIS100. DS345 of SIS18 is directly triggered by the 10 MHz of BuTiS receiver and DS345 of SIS100 is triggered by DS345 of SIS18. So both DS345s are synchronized to BuTiS. The B2B source SCU, B2B target SCU and trigger SCU are connected to the same WR switch, which connects to the timing network. PC[7] is used as a DM to produce the B2B start event. Besides, it monitors the status of the B2B transfer programs in all SCUs. The oscilloscope is used to monitor the alignment of the two simulated RF Reference Signals within the synchronization window provided by the trigger SCU.

Fig. 5.23 shows the front and back view of the test setup. DS345 of SIS18 produces the sine wave of 1.572 200 MHz frequency for the B2B source SCU. DS345 of SIS100 produces the sine wave of 1.572 000 MHz for the B2B target SCU. So the beating frequency is 200 Hz and the synchronization period is 5 ms.

[6] `http://www.thinksrs.com/downloads/PDFs/Manuals/DS345m.pdf`

[7] A Linux personal computer is installed with the standard TR tools and library. `https://www-acc.gsi.de/wiki/Timing/TimingSystemNodesCurrentRelease`

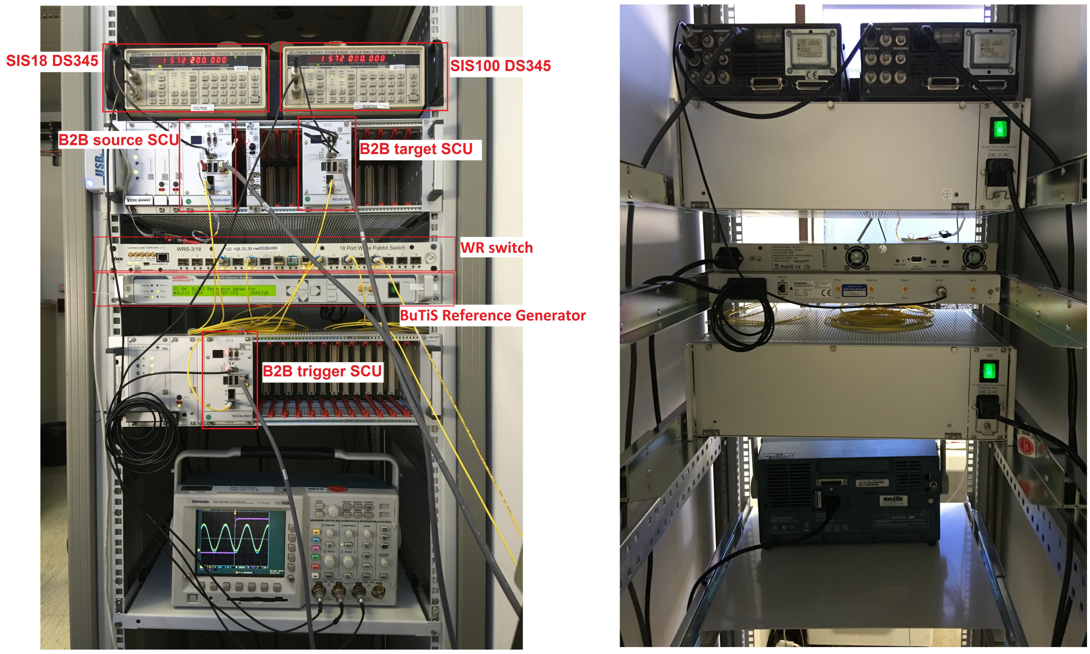

Abbildung 5.23: The front and back view of the test setup

5.4.3 The firmware of the B2B transfer system

The B2B source, B2B target and trigger SCUs have different firmware running on their soft CPU, LM32[8]. The firmware are activated by the B2B start timing frame, *CMD_START_B2B*, which indicates the source and target synchrotrons of the B2B transfer.

- Firmware for the B2B source SCU

  The firmware for the B2B source SCU is the core program of the B2B transfer system. See Fig. 5.24.

  - Step 1. The program waits for the CMD_START_B2B timing frame.
  - Step 2. When it receives the timing frame CMD_START_B2B, it collects the predicted phase and checks whether it is within a proper range of 0° to 360°. If not, it sends a timing frame TGM_B2B_ERROR to the WR network and goes back to the step 1, which indicates the data error.
  - Step 3. It waits for the TGM_PHASE_TIME timing frame from the B2B target SCU, which contains the predicted phase and the slop of the target synchrotron.
  - Step 4. When it receives the timing frame TGM_PHASE_TIME within a specified timeout interval, it calculates the synchronization window, the phase shift/jump value and the phase correction value. Or it sends a timing frame TGM_B2B_ERROR to the WR network and goes back to the step 1, which indicates the timeout error of the frame. Besides, it checks whether the phase correction is in the range of 0° to 360° ,

[8]LatticeMico32 is a 32-bit microprocessor soft core from Lattice Semiconductor optimized for field-programmable gate arrays (FPGAs).

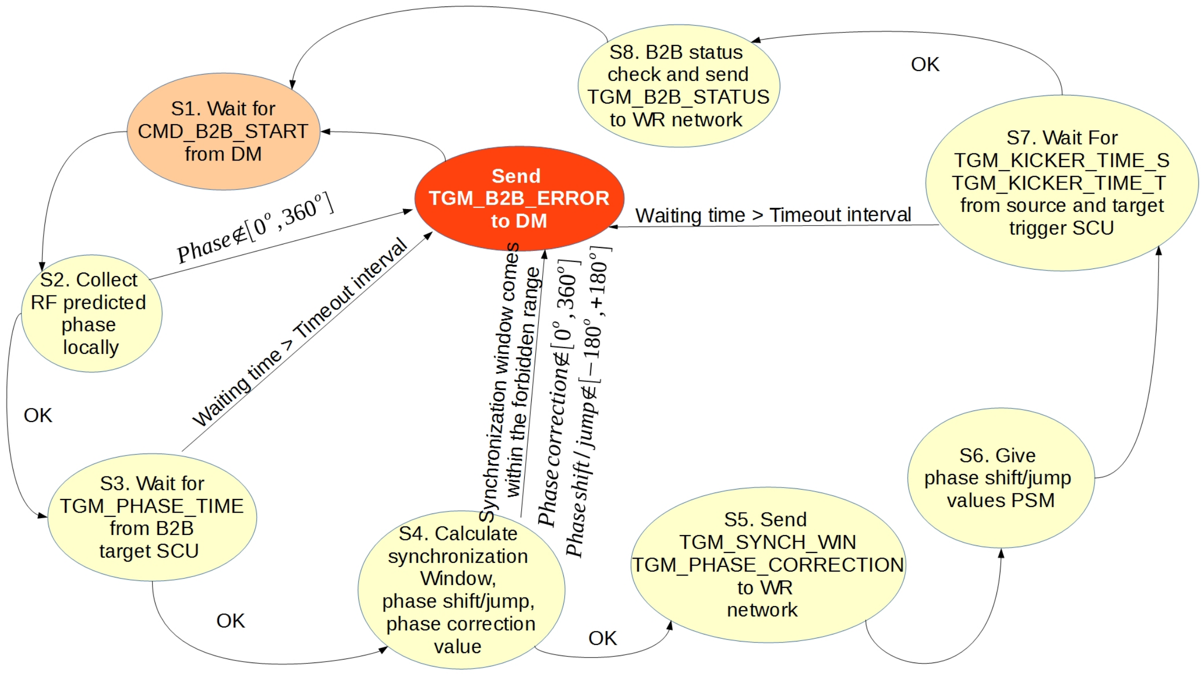

Abbildung 5.24: Flow chart of the firmware for B2B source SCU. Step is represented as S in the figure.

the required phase shift in the range of -180° to 180° and the start of the synchronization window not in the forbidden range. If at least one of them is not correct, it sends a timing frame TGM_B2B_ERROR to the WR network and goes back to the step 1, which indicates the calculation error.

- Step 5. It sends the timing frame TGM_SYNCH_WIN and TGM_PHASE_CORRECTIO to the WR network. TGM_SYNCH_WIN indicates the start of the synchronization window and TGM_PHASE_CORRECTION is used for the trigger SCUs for the reproduction of the bucket label signal.
- Step 6. It gives the phase correction and phase shift/jump values to corresponding modules.
- Step 7. It waits for the timing frame TGM_KICKER_TIME_S from the source trigger SCU and TGM_KICKER_TIME_T from the target trigger SCU, which contains the extraction/injection kicker trigger and firing timestamp. When it does not receive the timing frames within a specified timeout interval, it sends a timing frame TGM_B2B_ERROR to the WR network and goes back to the step 1, which indicates the timeout error of the frame.
- Step 8. When it receives the timing frames mentioned in the step 7 within a specified timeout interval, it checks the B2B transfer status and sends TGM_B2B_STATUS to the WR network and goes to the step 1. The B2B transfer is successful, if the trigger time $<$ the firing time of the extraction kicker of the source synchrotron, the trigger time $<$ the firing time of the injection kicker of the target synchrotron and the firing time

of the extraction kicker < the firing time of the injection kicker. Or the B2B transfer is failure.

- Firmware for the B2B target SCU

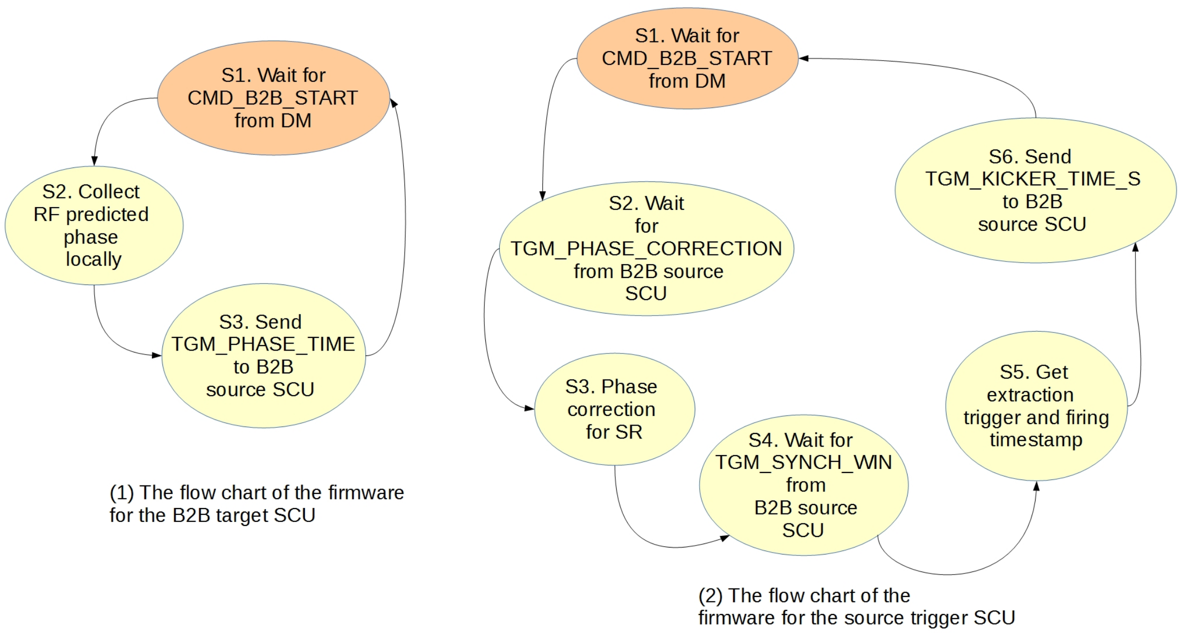

Abbildung 5.25: Flow chart of the firmware for B2B target SCU. Step is represented as S in the figure.

Fig. 5.25 (a) shows the flow chart of the program of the B2B target SCU.

- Step 1. The program waits for the CMD_START_B2B timing frame.
- Step 2. When it receives the timing frame CMD_START_B2B, it collects the predicted phase.
- Step 3. It sends the TGM_PHASE_TIME timing frame to the B2B source SCU and goes back to the step 1.

- Firmware for the trigger SCU

  Fig. 5.25 (b) shows the flow chart of the program of the source trigger SCU. For the target trigger SCU, the flow chat is same only with the different name of the timing frame TGM_KICKER_TIME_T.

- Step 1. The program waits for the CMD_START_B2B timing frame.
- Step 2. The program waits for the TGM_PHASE_CORRECTION timing frame.
- Step 3. The program gives the phase correction value to the corresponding module for the bucket label signal reproduction.

- Step 4. When it receives the timing frame CMD_START_B2B, it waits for the timing frame TGM_SYNCH_WIN to indicate the synchronization window for the kicker trigger.
- Step 5. After the beam extraction, it collects the trigger and firing timestamp.
- Step 6. It sends the TGM_KICKER_TIME_S timing frame to the B2B source SCU and goes back to the step 1.

5.4.4 The time constraints of the B2B transfer system

For the B2B transfer system, the time constraints are very important and strict. Fig. 5.26 shows the time constraint of the system. The CMD_START_B2B is executed at t_{B2B}. The RF phase prediction needs 500 µs, so the B2B source and target SCUs collect the phase data at t_{B2B} + 500 µs and need about 450 ns for the data collection. The B2B source SCU receives the timing frame TGM_PHASE_TIME at around t_{B2B} + 500 µs + 450 ns + 500 µs ≈ t_{B2B} + 1 ms. The second 500 µs is the latency of the WR network. After that, the B2B source SCU needs about 100 µs for the calculation, the timing frame TGM_SYNCH_WIN and TGM_PHASE_CORRECTION sending and data transferring to the corresponding module. TGM_SYNCH_WIN is sent at around t_{B2B} + 1 ms + 100 µs ≈ t_{B2B} + 1.1 ms. The trigger SCU receives TGM_PHASE_CORRECTION and TGM_SYNCH_WIN at around t_{B2B} + 1.1 ms + 500 µs ≈ t_{B2B} + 1.6 ms. The 500 µs is the latency of the WR network. The start of the synchronization window must be later than t_{B2B} + 1.1 ms + 2×500 µs ≈ t_{B2B} + 2.1 ms, because the TGM_SYNCH_WIN must be transferred back to the DM and the DM transfers it further to the beam instrumentation devices via WR network. The upward to DM transfer needs maximum 500 µs and the transfer from the DM to BI needs another 500 µs. Because the upper bound B2B transfer time is 10 ms and there is no hard real time for the collection of the trigger and firing timestamps and timing frame TGM_KICKER_TIME_S sending, we give 1 ms for the source trigger SCU to do this task and the source trigger SCU sends TGM_KICKER_TIME_S at around t_{B2B} + 10 ms + 1 ms ≈ t_{B2B} + 11 ms. The same time constraints is also for the target trigger SCU. The B2B source SCU receives TGM_KICKER_TIME_S and TGM_KICKER_TIME_T at around t_{B2B} + 11 ms + 500 µs ≈ t_{B2B} + 11.5 ms. The 500 µs is the latency of the WR network. The B2B source SCU sends TGM_B2B_STATUS at around t_{B2B} + 11.5 ms + 100 µs ≈ t_{B2B} + 11.6 ms. The BI devices receives the timing frame TGM_B2B_STATUS at around t_{B2B} + 11.6 ms + 2×500 µs ≈ t_{B2B} + 12.6 ms.

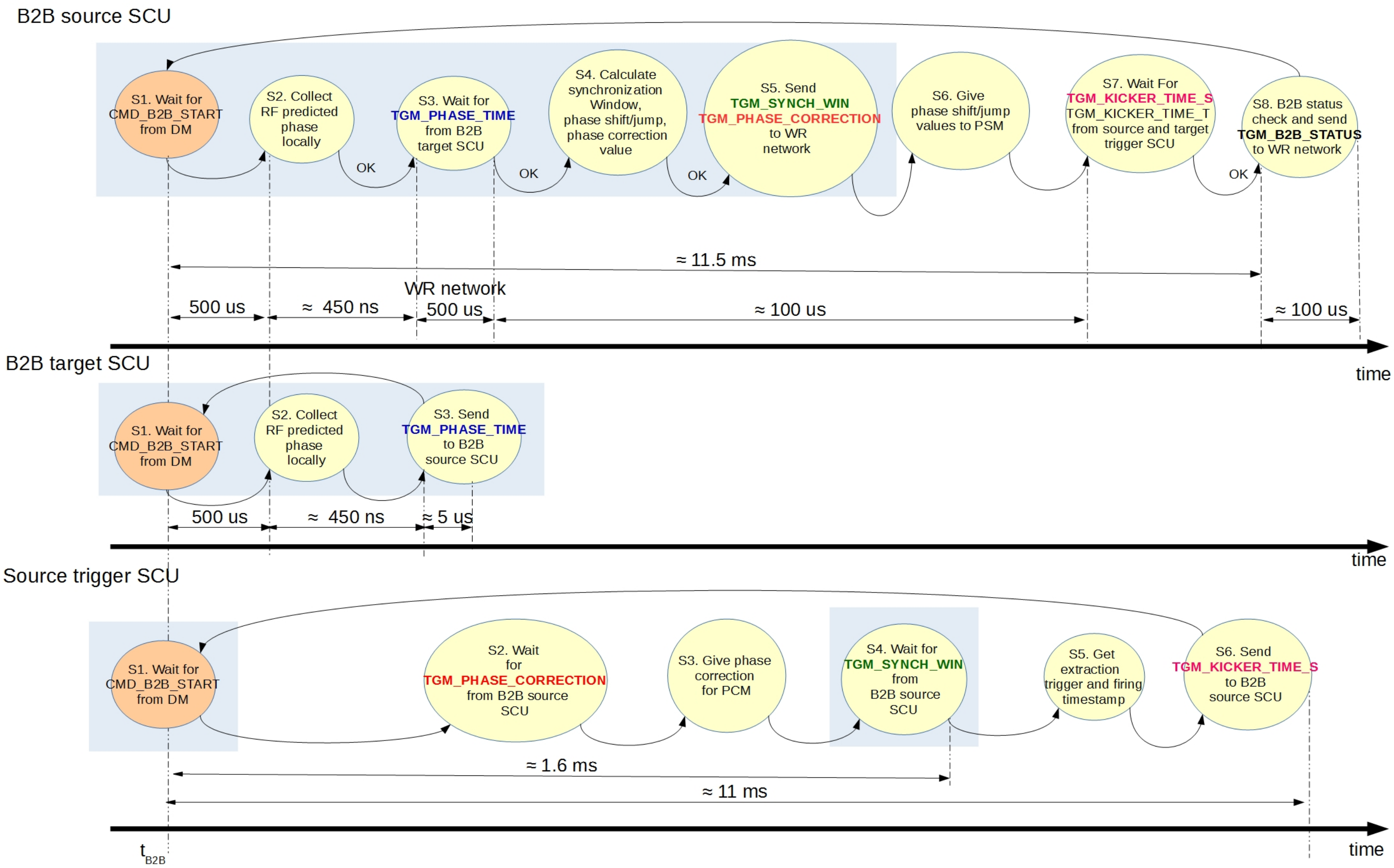

Abbildung 5.26: The time constraints of the B2B transfer system. The sent and received timing frame pairs have the same color. The test setup realizes the steps in the blue rectangle.

5.4.5 Test result

Because some modules of the B2B transfer system are still under the development, the test setup realizes parts of the whole function, mainly concentrated on the data collection from two simulated RF reference signals, the calculation of the synchronization window and the distribution of the start of the synchronization window. The steps with the blue rectangle in Fig. 5.26 are realized in this test setup. The test result of the B2B programs on B2B source, B2B target and trigger SCUs are shown as follows.

```

U28+ B2B transfer from SIS18 to SIS100 => Source B2B SCU
==================================================
SIS18: Frequency of the RF reference signal  = 1.572200MHz
SIS100: Frequency of the RF reference signal  = 1.572000MHz
SIS18: Period of the RF reference signal  = 636051(ps)
SIS100: Period of the RF reference signal  = 636132(ps)

>>>>>>>>>>>>>>>>>>>>>>>>> Receive CMD_START_B2B from WR network
Timestamp of the RF reference signal from SIS18 (accuracy to 1ns)
GMT: Thu, Jan 8, 1970, 21:07:27.445405856

>>>>>>>>>>>>>>>>>>>>>>>>> Receive TGM_PHASE_TIME from WR network
Timestamp of the RF reference signal from SIS100 (accuracy to 1ns)
GMT: Thu, Jan 8, 1970, 21:07:27.445364560

Beating time: 4.622818 (ms)
The number of the SIS18 revolution for the synchronization: 3634
Start of the synchronization window: GMT: Thu, Jan 8, 1970, 21:07:27.450028674

<<<<<<<<<<<<<<<<<<<<<<<<<< Send TGM_SYNCH_WIN to WR network
```

```

U28+ B2B transfer from SIS18 to SIS100 => Target B2B SCU
==================================================
>>>>>>>>>>>>>>>>>>>>>>>>> Receive CMD_START_B2B from WR network
Timestamp of the RF reference signal from SIS100 (accuracy to 1ns)
GMT: Thu, Jan 8, 1970, 21:07:27.445364560

<<<<<<<<<<<<<<<<<<<<<<<<<< Send TGM_PHASE_TIME to WR network
```

```

U28+ B2B transfer from SIS18 to SIS100 => Trigger SCU
==================================================
Waiting for timing events ...
>>>>>>>>>>>>>>>>>>>>>>>>> Receive TGM_SYNCH_WIN from
```

```
              WR network
6 Event execution timestamp: GMT 1970−01−08 21:07:27.450028674
```

After both B2B source and target programs receive the CMD_START_B2B frame, they trigger another unit connected to the System-on-Chip[9] (SoC) bus to get the timestamp of the next zero crossing point of the DS345 sine waves, which is simulated as an equivalent to the predicted phase. The triggers of the B2B source and target SCUs are not simultaneous, namely the B2B source and target SCU do not get the timestamp of the adjacent zero crossing points of two RF simulated sine signals, see Line 10 and 14 of the test result of the B2B source SCU. All timestamp are shown in the format of Greenwich Mean Time (GMT). The timestamp got by the B2B source SCU is Thu, Jan 8, 1970, 21:07:27 0.445405856 second and the timestamp got by the B2B target SCU is Thu, Jan 8, 1970, 21:07:27 0.445364560 second. The time difference between two timestamps is 41.296 µs. There are two reasons for the asynchronous triggers.

- The SoC bus might be granted to other program and B2B program must wait until it is free.
- The printout of the user friendly messages of the LM32 programs causes the non real time of the programs.

The difference between timestamps of the adjacent zero crossing points, 592ns, is the remainder resulting from 41.296us dividing SIS18 revolution period 636 051 ps. Based on eq. 5.52 and eq. 5.53,

$$\frac{T^{SIS18}_{h=2}}{5ms} = \frac{592ns}{\Delta t} \tag{5.52}$$

$$\frac{\Delta t}{T^{SIS18}_{h=1}} = 3634 \tag{5.53}$$

we could get that the beating time Δt is 4.622 818 ms and the number of the SIS18 revolution period is 3634 for the test.

For the real application of the B2B transfer system, in order to guarantee the time constraints of the B2B programs, see Fig. 5.26, the B2B source, target and trigger SCUs run only their corresponding B2B program. The SoC bus is occupied only by the B2B program. Besides, the programs running on LM32 are forbidden to print out any user friendly messages.

[9] A system-on-chip is an integrated circuit that integrates all components of a computer or other electronic system into a single chip.

Kapitel 6

Existing transfer system and the transfer system of the FAIR accelerators

6.1 Existing transfer from SIS18 to ESR

6.2 B2B transfer from SIS18 to ESR to CRYRING

Kapitel 7

Summary

Kapitel 8

Acknowledgement

I wish to express my sincere gratitude to Prof. Oliver Kester, David Ondreka and Dietrich Beck for their supervision, valuable guidance and helpful suggestions. I would like to express my sincere appreciation to Turgut «elikadam, for providing us VoIP device for our measurements. He also helped us for adding extra functions for delay measurements to VoIP device. And also I want to thank to Hasan «itÁ and my friends in ASELSAN Inc. for their valuable friendship, help and support. I want to thank to Şanser Şirin from Hacettepe University and Oktay KoÁ from Middle East Technical University for their help and support during measurements. And also I want to thank to Mehmet Celep, Alparslan Gˆzel and Halil İbrahim Seyrek from Gebze Institute of Technology for their help and support during measurements. I am also grateful to ASELSAN Inc. for facilities provided for the completion of this thesis. I am grateful to my wife, Esin, because she always supported me and cheered me up when I needed.

Anhang A

Formelzeichen

A.1 Konstanten

1. Elementarladung

$$1e = 1,6021766208(98) * 10^{-19}C$$

2. nächstes Geraffel

Anhang B

Messwerttabellen

Anhang C

Abbildungsverzeichnis

Literaturverzeichnis

[1] Dietrich Beck, R. Bar, Mathias Kreider, Cesar Prados, Stefan Rauch, Wesley Terpstra, and Marcus Zweig. The new White Rabbit based timing system for the FAIR facility. Proceedings of PCaPAC2012, Kolkata, India, 2012.

[2] Eizi Ezura, Masahito YOSHII, Fumihiko TAMURA, and Alexander SCHNASE. Beam-Dynamics View of RF Phase Adjustment for Synchronizing J-PARC RCS with MR or MLF, 2008.

[3] T. Hoffmann. FESA–The front-End Software architecture at FAIR. PCaPAC08, 2008.

[4] Harald Klingbeil, Ulrich Laier, Klaus-Peter Ningel, Stefan Schäfer, Christof Thielmann, and Bernhard Zipfel. New digital low-level rf system for heavy-ion synchrotrons. Physical Review Special Topics - Accelerators and Beams, 14(10), October 2011.

[5] S Y Lee. Accelerator Physics. WORLD SCIENTIFIC, Singapore, 3 edition, November 2011.

[6] Peter Moritz. BuTiS–Development of a Bunchphase Timing System. GSI Scientific Report, 2007, 2006.

[7] B. Zipfel, P. Moritz, and others. Recent Progress on the Technical Realization of the Bunch Phase Timing System BuTiS. Proc. IPAC, pages 418–420, 2011.